KfK 3173
EUR 7053e
Mai 1981

A Theoretical Study on the Growth of Large Sodium Vapor Bubbles in Liquid Sodium

F. Casadei
Institut für Neutronenphysik und Reaktortechnik
Projekt Schneller Brüter

Kernforschungszentrum Karlsruhe

KERNFORSCHUNGSZENTRUM KARLSRUHE

Institut für Neutronenphysik und Reaktortechnik

Projekt Schneller Brüter

KfK 3173
EUR 7053e

A Theoretical Study on the Growth of Large Sodium Vapor Bubbles in Liquid Sodium

F. Casadei*

*working with an Euratom grant at the Institut für Neutronenphysik und Reaktortechnik, Karlsruhe

Kernforschungszentrum Karlsruhe, GmbH., Karlsruhe

Kernforschungszentrum Karlsruhe GmbH
ISSN 0303-4003

Contents

5. Results

Acknowledgement

References

Figures

Abstract

The growth of a large sodium vapor HCDA bubble in a finite pool of cold sodium is modelled. During the growth the bubble is supplied with hot vapor coming from the core region through an orifice. Nonequilibrium at the phase interface is allowed, and the effect of noncondensable fission gases is parametrically studied.
Results are presented in graphical form for the case of a typical 300 MW fast breeder reactor. An increase of the quantity of noncondensable fission gases is showed to cause a slight increase of the growth velocity, and a much greater increase of the vapor temperature and decrease of the liquid interface temperature, as expected.

Theoretische Untersuchungen über das Wachstum von großen Natriumdampfblasen in flüssigem Natrium

Zusammenfassung

In dieser Arbeit wird das Wachstum einer großen HCDA-Natriumdampfblase im kalten flüssigen Natrium theoretisch untersucht. Während des Wachstums wird die Blase mit heißem Natriumdampf aus dem Kern gespeist. Temperaturdifferenzen an der Blasenoberfläche werden berücksichtigt und der Effekt von unkondensierbaren gasförmigen Spaltprodukten wird parametrisch untersucht. Es werden Ergebnisse für einen typsichen 300 MW-Schnellen Brüter dargestellt. Eine Zunahme der Konzentration der unkondensierbaren Gase verursacht eine geringe Zunahme der Wachstumsgeschwindigkeit und eine viel größere Zunahme der Dampftemperatur und Abnahme der Temperatur des flüssigen Natriums an der Blasenoberfläche.

Latin symbols:

a	coefficient
A	expression (3.22)
b	coefficient
B	expression (2.58)
c	Condensation-evaporation Coefficient (-); coefficient (-)
C	expression (3.21)
c_1, c_2, c_3	coefficients
c_p	specific heat at constant pressure (J/kg • k)
c_v	specific heat at constant volume (J/kg.k)
D	liquid thermal diffusivity (m^2/sec)
E	energy per unit surface (J/m^2)
E'	energy per unit surface (J/m^2)
f	function
$F, \overline{F}$	function
h	enthalpy (J), time step (sec)
$\hat{h}_{ev}$	specific vaporization enthalpy at $T=T_L$ (J/kg)
$\hat{h}^*_{L,liq.}$	specific enthalpy of saturated liquid at $T=T_L$ (J/kg)
$\hat{h}^*_{L,vap}$	specific enthalpy of saturated vapor at $T=T_L$ (J/kg)
$\hat{h}_v$	specific enthalpy of vapor at $T=T_v$, $p=p_v$ (J/kg)
I	Plesset-Zwick integral
K	thermal conductivity (J/sec•m•k)
K_1, K_2, K_3, K_4	expressions (4.10) used in Runge-Kutta integration
M	mass (kg)
M_{ev}	evaporated mass (kg/m^2)
M_{co}	condensed mass (kg/m^2)
$\dot{M}_{in}$	mass flow rate introduced from the source into the bubble (kg/sec)
M_W	Sodium molar weight (kg/mol)
n	exponent
p	pressure (N/m^2)

p'	sum of all the normal stresses (N/m^2)
p_L^*	sodium saturation pressure at $T=T_L$ (N/m^2)
r	radial coordinate (m)
R	bubble radius (m)
R'	external liquid radius (m)
R_g	perfect gas constant ($J/mol \cdot K$)
R_L	boundary layer external radius (m)
S	Orifice cross section (m^2)
t	time (sec)
T	absolute temperature (K)
u	radial velocity (m/sec)
$\hat{v}$	specific volume (m^3/kg)
V	volume (m^3)
W	work made by the vapor against the liquid (J)
x	integration variable (sec)
y	integration variable (sec), prediction corrector variable
y_R	velocity of expansion of the bubble (m/sec)

Greek letters:

γ	adiabatic exponent
δ	boundary layer thickness (m)
μ	dynamic viscosity ($kg/m \cdot s$)
Π	3.1415
ρ	density (kg/m^3)
σ	surface tension (N/m)
τ	Plesset-Zwick variable, defined by (2.77), ($m^4 \cdot$ sec)
ζ, ζ', ζ''	Plesset-Zwick variable ($m^4 \cdot$ sec)

Superscripts:

.	time derivative (1,s)
*	saturated conditions
∧	specific quantity (1/kg)

Subscripts:

c	of cover gas
co	condensation
crit	critical
ev	evaporation
i	in the vapor source
in	introduced from the source to the bubble
l	of liquid
L	of liquid, at the interface
lin	linearized
m	index
R	at radius r=R
v	of vapor
vl	from vapor to liquid
0	initial
2	final
∞	at infinity

List of Figures:

List of Tables:

1. Introduction

1.1 Description of the problem

The dynamics of the expansion of large bubbles of hot sodium vapor in a pool of relatively cold liquid sodium plays an important role in understanding the effects of an hypothetical core-disruptive accident (HCDA) in Liquid Metal Fast Breeding Reactors (LMFBR-s). As a result of fuel-coolant interaction in an HCDA, a large bubble would be formed by the discharge of a mixture of hot sodium vapor, liquid sodium, highly dispersed fuel and fission gases, from the core region into the relatively cold liquid sodium pool placed above the core.

An isentropic expansion of the bubble down to the equilibrium pressure, taking into account the compression of the cover gas volume, would be a rather simple but too conservative estimate, i.e. overestimate ., of the work performed by the bubble.

The work potential of the accident is much mitigated, if heat transfer to the cold liquid pool, mainly due to condensation of hot sodium vapor at the bubble surface, is taken into account.

On the other hand, this mitigating effect could be seriously reduced by the presence of the noncondensable fission gases, which tend to accumulate near the condensation surfaces, inhibiting the heat transfer.

Other mechanisms , such as cold liquid sodium entrainment in the bubble, the presence of relatively cold structures in the pool etc., can influence the bubble expansion as well, generally, but not always, in the sense of mitigating the work potential. They have not been considered in the present approach.

1.2 Previous work

The literature on bubble dynamics that we have examined, can be roughly divided into two major classes, the first dealing with boiling and growth of small bubbles in superheated liquids, the second with expansion and collapse at large bubbles surrounded by

relatively cold liquid, mainly for HCDA simulation.

To the first class belong classical papers like those of Plesset and Zwick /1,11,12/,of Birkhoff and Margulies /15/, of Theofanous and Fauske /3/, of Bornhorst and Hatsopoulos /13, 14/. More recently,studies have been performed by Dalle Donne and Ferranti /16/, Brook and Mills /5/ and Prosperetti and Plesset/17/.

To the second class belong the paper of Reynolds and Kennedy/18/ who examined the condensation of a large sodium vapor bubble obtained by adiabatic expansion of the products of a typical HCDA, while it rises in the liquid sodium pool, assuming a constant condensation heat transfer coefficient. The condensation process was found to be governed by transient conduction in the liquid and a significant fraction of the sodium vapor was concluded to condense before the bubble reaches the pool surface. A subsequent paper of Theofanous and Fauske /19/ once more analyzed the condensation of a rising bubble, but taking into account the effect of noncondensables and solving the problem of transient mass diffusion in the vapor space in conjunction with the transient heat conduction and convection in the liquid phase. The presence of noncondensables was found to seriously delay the condensation process.

The paper by Özişik and Kress /20/ treats the problem of the condensation of the rising bubble in a way similar to the previous work /19/, i.e. including the effect of fission gases, but a turbulent boundary layer is assumed, rather than transfer by molecular diffusion in the vapor phase. The reason of this modification is that a diffusion model may underestimate the condensation rates if strong internal convection motions are present.

Finally Reynolds and Berthoud /4/ have analyzed both theoretically and experimentally the expansion and collapse of large two phase (water vapor and liquid water) bubbles in a pool of cold liquid water. The effect of noncondensables was not included.
An early instability of the bubble surface was observed. During this phase conduction-limited heat transfer is shown to be too slow to account for the experimental results, while it describes

well the bubble expansion and collapse as soon as the bubble surface becomes stable. The heat and mass transfer, in the absence of non-condensable gases, significanty mitigates the mechanical work.

1.3 Present model and assumptions

The present model describes the expansion and collapse of a large sodium vapor bubble in a finite pool of relatively cold liquid sodium. During its growth the bubble is supplied with hot sodium vapor coming from the core region. The core region is modelled with a superheated vapor source at constant pressure and temperature, connected with the bubble through an orifice. The discharge of hot sodium vapor through the orifice is governed by the pressure difference between core region and bubble. The geometry of the problem is spherical (see Fig. 1).

The temperature and the pressure of the vapor in the bubble are considered to be uniform. The mass of liquid contained in the pool is finite. The presence of the cover volume is also modelled by means of an external spherical gas shell which may be compressed by the motion of the liquid.
The reactor tank is considered to be rigid and is modelled by an external rigid boundary.
The initial conditions are as follows: the bubble has an initial radius of 0.1 m., is filled with sodium saturated vapor at atmospheric pressure, i.e. at about 1154K, and the sodium pool, containing 110 m^3 of liquid, has an initial uniform temperature of 800K.
The initial temperature at the interface is also 800K. A 70 m^3 cover gas volume surrounds the liquid. The volumes and temperatures chosen are typical of a 300 MW fast breeder reactor.
The hot sodium vapor in the core region has a constant pressure of 5 bar and a constant temperature of 1700K. The orifice connecting the bubble with the source starts to open linearly at t=0 and is completely open after 1 msec. Orifice parameters are so chosen that a maximum mass injection rate of 100 kg/sec of hot vapor from the core is reached. Nonequilibrium between the sodium vapor in the bubble and the liquid at the interface is described by the model, since the temperature of the vapor is different from the temperature of the liquid at the wall.

The effect of noncondensable fission gases on the expansion and collapse of the bubble is modelled by introducing condensation and evaporation coefficients, a technique used in many previous works /3,4,5/. A parametric study is made varying the value of the coefficients according to experimental data.
The interphase heat transfer problem is solved together with the heat conduction in the liquid and the liquid motion problem.

Two distinct models are presented, the difference beeing only in the description of the heat conduction in the liquid.
The first model uses the Plesset-Zwick /1/ solution for the heat diffusion across a spherical boundary with radial motion.
The second uses the Theofanous-Fauske /3/ technique of solving the energy equation for the liquid by postulating a thin second order thermal boundary layer in the liquid.
Only the results obtained by the first method are shown in the present report. Calculations were made also using the second approach. The results of these are not presented here, as they are in full agreement with the previous ones.
The presence of liquid sodium, of fuel particles and fuel vapor in the bubble, the entrainment of liquid drops from the pool, the presence of cold structures and the instability of the bubble surface are neglected at the present stage of the model.
Rising of the bubble in the pool is also neglected, since the expansion characteristic times are much smaller than the time required to rise in the pool.

1.4 Differences between the present model and the previous approaches

The main differences between the present model and the previous approaches can be resumed as follows:

a) instead of considering a constant-radius rising bubble, as in /18, 19, 20/ we investigate the expansion phase of the bubble.

b) we simulate the flow of hot sodium vapor from the core during the expansion, instead of modelling a flashing water source like in /4/.

2. Governing equations using the Plesset-Zwick solution

2.1 Continuity equation for the liquid

Let us consider an incompressible fluid, for which:

$$\rho_l = \text{const.} \tag{2.1}$$

The continuity equation in spherical coordinates and in presence of a spherical symmetry is then:

$$\frac{\partial}{\partial r}\left(r^2 u\right) = 0. \tag{2.2}$$

Expanding the derivative one gets:

(2.3) $$\frac{\partial u}{\partial r} = -2\frac{u}{r}.$$

and from (2.3):

(2.4) $$\frac{\partial}{\partial r}\left(r^2\frac{\partial u}{\partial r}\right) = 2u.$$

(2.5) $$\frac{\partial^2 u}{\partial r^2} = 6\frac{u}{r^2}.$$

which will be used in the following sections.

Eq, (2.2) can also be rewritten as:

(2.6) $$r^2 u = R^2\dot{R}.$$

or

(2.7) $$u = R^2\dot{R}/r^2.$$

2.2 Equation of motion for the liquid:

The equation of motion of a viscous, incompressible fluid (Navier-Stokes' equation) /9/ in spherical coordinates and in presence of a spherical symmetry is

(2.8) $$\frac{\partial u}{\partial t} + u\frac{\partial u}{\partial r} = -\frac{1}{\rho_l}\frac{\partial p'}{\partial r} + \frac{\mu_l}{\rho_l}\left[\frac{1}{r^2}\frac{\partial}{\partial r}\left(r^2\frac{\partial u}{\partial r}\right) - 2\frac{u}{r^2}\right].$$

where

(2.9) $$p' = p + 2\mu_l\frac{\partial u}{\partial r}.$$

represents the sum of all the normal stresses, and is given by the static pressure plus the normal friction stresses.

From Eq. (2.4) one gets:

(2.10) $$\frac{1}{r^2}\frac{\partial}{\partial r}\left(r^2\frac{\partial u}{\partial r}\right) - 2\frac{u}{r^2} = 0.$$

and from Eq. (2.5), (2.9) :

(2.11) $$\frac{\partial p'}{\partial r} = \frac{\partial p}{\partial r} + 12\mu_l\frac{u}{r^2}.$$

Using Eq. (2.3), (2.10), (2.11) , Eq. (2.8) becomes:

$$\frac{\partial u}{\partial t} - 2\frac{u^2}{r} = -\frac{1}{\rho_\ell}\frac{\partial p}{\partial r} - 12\frac{\mu_\ell}{\rho_\ell}\frac{u}{r^2}. \tag{2.12}$$

From Eq. (2.7) one gets then:

$$\frac{\partial u}{\partial t} = \frac{1}{r^2}\left(\ddot{R}R^2 + 2R\dot{R}^2\right). \tag{2.13}$$

Substituting now Eq. (2.7), (2.13) in(2.12) one obtains the equation of motion of the liquid in the final form:

$$\frac{\ddot{R}R^2 + 2R\dot{R}^2}{r^2} - 2\frac{R^4\dot{R}^2}{r^5} = -\frac{1}{\rho_\ell}\frac{\partial p}{\partial r} - 12\frac{\mu_\ell}{\rho_\ell}\frac{R^2\dot{R}}{r^4}. \tag{2.14}$$

This equation is now integrated with respect to the radial coordinate r from the bubble radius R to a general radius r_2. With the assumption (2.1) and assuming that the viscosity of the liquid is also constant:

$$\mu_\ell = \text{const}. \tag{2.15}$$

the integration yields:

$$\left(\ddot{R}R^2 + 2R\dot{R}^2\right)\cdot\left(\frac{1}{R} - \frac{1}{r_2}\right) - \frac{1}{2}R^4\dot{R}^2\left(\frac{1}{R^4} - \frac{1}{r_2^4}\right) = \tag{2.16}$$

$$= -\frac{1}{\rho_\ell}\left(p_2 - p_R\right) - 4\frac{\mu_\ell}{\rho_\ell}R^2\dot{R}\left(\frac{1}{R^3} - \frac{1}{r_2^3}\right).$$

The pressure p_R of the liquid at the bubble boundary can be expressed by:

$$p_R = p_v - 2\frac{\sigma}{r} . \tag{2.17}$$

Now we have to distinguish between two different cases: in the first case, considering the expansion of a vapor bubble in a very large pool of liquid, as it can be in the case of bubble growth in superheated liquid, we have to set:

$$r_2 \longrightarrow \infty .$$
$$p_2 = p_\infty . \tag{2.18}$$

and eq. (2.16), using (2.17), reduces to:

$$\ddot{R}R + \frac{3}{2}\dot{R}^2 + 4\frac{\mu_l}{\rho_l}\frac{\dot{R}}{R} + 2\frac{\sigma}{\rho_l}\frac{1}{R} = \frac{p_v - p_\infty}{\rho_l} . \tag{2.19}$$

In the second case, considering the expansion of a large vapor bubble in a finite liquid pool, see Fig.(1), we have to consider the external radius R' of the liquid pool and to set p_2 equal to the pressure of the cover gas, i.e.:

$$r_2 = R' .$$
$$p_2 = p_c . \tag{2.20}$$

For (2.1), the external liquid radius R' can be given as a function of R by:

$$R' = \left(\frac{3}{4\pi}V_l + R^3\right)^{1/3} . \tag{2.21}$$

The pressure of the cover gas volume, p_c, can be expresssed as a function of R if we assume that the cover gas is adiabatically compressed by the expansion of the bubble

$$p_c = p_{c,o} \cdot \left[\frac{1-(R_o'/R_c)^3}{1-(R'/R_c)^3}\right]^{\gamma_c} . \tag{2.22}$$

If the reactor tank is considered to be rigid one has simply

$$R_c = \left(\frac{3}{4\pi} V_{c,o} + R_o'^3\right)^{1/3} = \text{const.} \tag{2.23}$$

where

$$R_o' = \left(\frac{3}{4\pi} V_l + R_o^3\right)^{1/3} . \tag{2.24}$$

Eq. (2.16) can be rewritten in this case as:

$$\left(R - \frac{R^2}{R'}\right)\cdot\ddot{R} + \left(\frac{3}{2} - 2\frac{R}{R'} + \frac{1}{2}\frac{R^4}{R'^4}\right)\cdot\dot{R}^2 + \left[4\frac{\mu_l}{\rho_l}\left(\frac{1}{R} - \frac{R^2}{R'^3}\right)\right]\cdot\dot{R} - \frac{1}{\rho_l}\left(p_v - 2\frac{\sigma}{R} - p_c\right) = 0. \tag{2.25}$$

where R' and p_c are given by (2.21) to (2.24).

2.3 Energy equation for the liquid

The problem of the heat diffusion across a spherical boundary with radial motion has been analytically solved in successive approximations by Plesset and Zwick /1/. The approximation procedure converges rapidly, provided the temperature variations are appreciable only in a thin layer adjacent to the spherical boundary. Here the zero-order solution is used, without higher-order corrections.
The explicit solution for the liquid temperature at the boundary is given in the zero order as a function of the temperature at infinity and of the temperature gradient at the spherical boundary:

$$T_L(t) = T_\infty - \left(\frac{D_l}{\pi}\right)^{1/2} \int_0^\tau \frac{(\partial T/\partial r)_R}{R^2 (\tau - \zeta)^{1/2}} \cdot d\zeta . \tag{2.26}$$

where

$$\tau = \int_0^t R^4(t) \cdot dt . \tag{2.27}$$

Substituting (2.27) into (2.26) one gets also:

$$T_L(t) = T_\infty - \left(\frac{D_l}{\pi}\right)^{1/2} \int_0^t \frac{R^2(x) \cdot (\partial T/\partial r)_R}{\left\{\int_x^t R^4(y) \cdot dy\right\}^{1/2}} \cdot dx . \tag{2.28}$$

2.4 Equation of mass transfer at the interface

The mass transport across a phase interface has been described in previous work /2/. The relationships used here are:

$$\dot{M}_{vl} = \dot{M}_{co} - \dot{M}_{ev} \quad . \tag{2.29}$$

where

$$\dot{M}_{co} = c_{co} \cdot \sqrt{\frac{M_w}{2\pi R_g}} \cdot \frac{p_v}{\sqrt{T_v}} \quad . \tag{2.30}$$

$$\dot{M}_{ev} = c_{ev} \cdot \sqrt{\frac{M_w}{2\pi R_g}} \cdot \frac{p_L^*(T_L)}{\sqrt{T_L}} \quad . \tag{2.31}$$

The relationships are similar to those used in previous literature /3, 4, 5/. The coefficients c_{co}, c_{ev} represent the ratio of the actual mass transfer to the value derived from the kinetic theory. Here a parametric study is made where these coefficients are varied between 1 and 0.01, a range which encompasses the large scatter of experimental data from the literature /3/.

2.5 Equations of energy transfer at the interface

The net rate of heat transfer at the interface is given by:

$$\dot{E}_{vl} = \dot{M}_{co} \cdot \hat{h}_v - \dot{M}_{ev} \cdot \hat{h}^*_{L,v} \quad . \tag{2.32}$$

This expression is used only in the energy balance for the vapor phase. The net rate of energy transmitted to the liquid phase is given by

$$\dot{E}'_{vl} = \dot{M}_{co} \cdot \left(\hat{h}_v - \hat{h}^*_{L,l}\right) - \dot{M}_{ev} \cdot \hat{h}_{lv} \quad . \tag{2.33}$$

which is slightly different from (2.32), due to the fact that the solution (2.26) given by Plesset and Zwick /1/ neglects the variation of mass of the liquid.
The heat transfer equation at the phase boundary (2.33) is then coupled with the heat diffusion solution in the liquid (2.26),(2.27) by taking for the temperature gradient at the boundary:

$$\left(\frac{\partial T}{\partial r}\right)_R = -\frac{\dot{E}'_{ve}}{K_l} \quad . \tag{2.34}$$

2.6 Vapor source description

The bubble is imagined to be connected with a vapor source through an orifice. The source contains sodium vapor at high pressure and temperature and is assumed to be so large that

$$p_i = \text{const.}$$
$$T_i = \text{const.} \tag{2.35}$$

,although a finite quantity of vapor flows from the source into the bubble. The critical pressure for the flow through the orifice is defined by:

$$p_{crit} = p_i \cdot \left(\frac{2}{n+1}\right)^{\frac{n}{n-1}} \quad . \tag{2.36}$$

where

$$n = \frac{c_{p,i}}{c_{v,i}} \quad . \tag{2.37}$$

The mass flow rate through the orifice is regulated by the downstream pressure, which is the pressure in the bubble. The maximum velocity in the orifice is the critical velocity. If the pressure in the bubble is

$$p_v \leq p_{crit} \quad . \tag{2.38}$$

then the critical velocity is reached and the mass flow rate from the source into the bubble is given by:

$$\dot{M}_{in} = \dot{M}_{in,crit} = S \cdot \sqrt{\frac{p_i}{\hat{v}_i} n \left(\frac{2}{n+1}\right)^{\frac{n+1}{n-1}}} \quad . \tag{2.39}$$

If the vapor pressure in the bubble exceeds the critical pressure:

$$p_v > p_{crit} \quad . \tag{2.40}$$

then the mass flow rate is given by

$$\dot{M}_{in} = S \cdot \sqrt{2 \frac{p_i}{\hat{v}_i} \frac{n}{n-1} \left[\left(\frac{p_v}{p_i}\right)^{\frac{2}{n}} - \left(\frac{p_v}{p_i}\right)^{\frac{n+1}{n}}\right]} \quad . \tag{2.41}$$

The cross section S of the orifice is calculated in order to produce a certain value of $\dot{M}_{in,crit}$,given as input.

2.7 Continuity equation for the vapor

The mass balance for the vapor contained in the bubble can be written as:

$$\dot{M}_v = \dot{M}_{in} - 4\pi R^2 \dot{M}_{vl} \quad . \tag{2.42}$$

This can be written as:

$$\frac{d}{dt}\left(\frac{4}{3}\pi R^3 \rho_v\right) = \dot{M}_{in} - 4\pi R^2 \dot{M}_{vl} \quad . \tag{2.43}$$

Performing the derivative and rearranging:

$$\rho_v \frac{dR}{dt} + \frac{R}{3}\frac{d\rho_v}{dt} + \dot{M}_{vl} - \frac{\dot{M}_{in}}{4\pi R^2} = 0. \tag{2.44}$$

The derivative of the vapor density is now expressed by

$$\frac{d\rho_v}{dt} = \frac{\partial \rho_v}{\partial T_v}\frac{dT_v}{dt} + \frac{\partial \rho_v}{\partial p_v}\frac{dp_v}{dt} . \tag{2.45}$$

Replacing (2.45) in (2.44) one gets finally:

$$\rho_v \frac{dR}{dt} + \frac{R}{3}\frac{\partial \rho_v}{\partial T_v}\frac{dT_v}{dt} + \frac{R}{3}\frac{\partial \rho_v}{\partial p_v}\frac{dp_v}{dt} + \dot{M}_{vl} - \frac{\dot{M}_{in}}{4\pi R^2} = 0. \tag{2.46}$$

where $\dot{M}_{vl}$ is given by (2.29) to (2.31) and $\dot{M}_{in}$ is given by (2.38) to (2.41)

2.8 Energy equation for the vapor

The energy balance for the vapor contained in the bubble can be written as:

$$\dot{E}_v = \dot{E}_{in} - \dot{W} - 4\pi R^2 \dot{E}_{vl} . \tag{2.47}$$

The work made by the vapor against the liquid is given by

$$\dot{W} = 4\pi R^2 \cdot p_v \cdot \frac{dR}{dt} \tag{2.48}$$

while the energy introduced by the vapor coming from the source is

$$\dot{E}_{in} = \dot{M}_{in} \cdot \hat{h}_i . \tag{2.49}$$

Eq. (2.47) can be rewritten as:

$$\frac{d}{dt}\left[\frac{4}{3}\pi R^3 \rho_v \hat{h}_v\right] = -4\pi R^2 \dot{E}_{vl} - 4\pi R^2 p_v \frac{dR}{dt} + \dot{M}_{in} \cdot \hat{h}_i \quad . \tag{2.50}$$

expanding the derivative and using Eq. (2.43) one gets:

$$\hat{h}_v \left[\dot{M}_{in} - 4\pi R^2 \cdot \dot{M}_{vl}\right] + \frac{4}{3}\pi R^3 \rho_v \frac{d\hat{h}_v}{dt} = \tag{2.51}$$

$$= -4\pi R^2 \cdot \dot{E}_{vl} - 4\pi R^2 p_v \frac{dR}{dt} + \dot{M}_{in} \cdot \hat{h}_i \quad .$$

The derivative of the vapor enthalpy can be expressed as:

$$\frac{d\hat{h}_v}{dt} = \frac{\partial \hat{h}_v}{\partial T_v} \cdot \frac{dT_v}{dt} + \frac{\partial \hat{h}_v}{\partial p_v} \cdot \frac{dp_v}{dt} \quad . \tag{2.52}$$

Substituting (2.52) into (2.51) and rearranging one finally obtains:

$$p_v \cdot \dot{R} + \frac{R}{3} \rho_v \frac{\partial \hat{h}_v}{\partial T_v} \dot{T}_v + \frac{R}{3} \rho_v \frac{\partial \hat{h}_v}{\partial p_v} \dot{p}_v + \tag{2.53}$$

$$+ \frac{\dot{M}_{in}}{4\pi R^2}\left(\hat{h}_v - \hat{h}_i\right) - \dot{M}_{vl} \cdot \hat{h}_v + \dot{E}_{vl} = 0 .$$

where $\dot{M}_{in}$ is given by (2.38) to (2.41), $\dot{M}_{vl}$ by (2.29) to (2.31) and $\dot{E}_{vl}$ by (2.32).

2.9 Final form of the differential equations

The problem of the bubble growth is completely described by the following equations:

a) Equation of motion for the liquid, Eq. (2.25)
b) Continuity equation for the vapor, Eq. (2.46)
c) Energy equation for the vapor, Eq. (2.53)
d) Energy equation solution for the liquid, Eq. (2.28)

The first three equations form the system of differential equations to be solved, simultaneously with the fourth expression which gives the liquid temperature at the interface.
The first equation, Eq. (2.25), is of the second order, and can be splitted into two equations of the first order. Let us define:

(2.54) $$y_R = \dot{R}$$

Eq. (2.25) becomes, using (2.54) and rearranging:

(2.55) $$\dot{y}_R = \frac{R'}{R(R'-R)} \left\{ -\frac{1}{2}\left[3 - 4\frac{R}{R'} + \left(\frac{R}{R'}\right)^4\right] \cdot y_R^2 + \right.$$
$$\left. -\left[4\frac{\mu_\ell}{\rho_\ell}\left(\frac{1}{R} - \frac{R^2}{R'^3}\right)\right] \cdot y_R + \frac{1}{\rho_\ell}\left(p_v - 2\frac{\sigma}{R} - p_c\right)\right\} .$$

From Eq. (2.46), using (2.54), one gets

(2.56) $$\dot{p}_v = \frac{3}{R\,\frac{\partial \rho_v}{\partial p_v}} \left[\frac{\dot{M}_{in}}{4\pi R^2} - \dot{M}_{v\ell} - \rho_v y_R - \frac{R}{3}\frac{\partial \rho_v}{\partial T_v}\dot{T}_v\right] .$$

Substituting (2.56) in Eq. (2.53), using (2.54) and rearranging one gets finally:

$$\dot{T}_v = \frac{1}{B}\left\{-p_v y_R - \rho_v \frac{\partial \hat{h}_v}{\partial p_v}\frac{1}{\frac{\partial \rho_v}{\partial p_v}}\left[\frac{\dot{M}_{in}}{4\pi R^2} - \dot{M}_{ve} - \rho_v y_R\right] + \right.$$

$$\left. - \frac{\dot{M}_{in}}{4\pi R^2}\left(\hat{h}_v - \hat{h}_i\right) + \dot{M}_{ve}\cdot \hat{h}_v - \dot{E}_{ve}\right\}. \tag{2.57}$$

where

$$B = \frac{R}{3}\rho_v\left(\frac{\partial \hat{h}_v}{\partial T_v} - \frac{\partial \hat{h}_v}{\partial p_v}\frac{1}{\frac{\partial \rho_v}{\partial p_v}}\frac{\partial \rho_v}{\partial T_v}\right). \tag{2.58}$$

Equations (2.54), (2.55), (2.57), (2.56) together with the solution (2.26) of the energy equation of the liquid form the system of five differential equations in the five unknown functions R, Y_R, T_v, p_v, T_L, which has to be solved.
In Table 1 all the equations and the formulas necessary for the solution of the problem are listed.

Summary of the governing equations using the Plesset-Zwick solution

(2.54) $$\dot{R} = y_R$$

(2.55) $$\dot{y}_R = \frac{R'}{R(R'-R)}\left\{-\frac{1}{2}\left[3 - 4\frac{R}{R'} + \left(\frac{R}{R'}\right)^4\right]\cdot y_R^2 + -\left[4\frac{\mu_l}{\rho_l}\left(\frac{1}{R} - \frac{R^2}{R'^3}\right)\right]\cdot y_R + \frac{1}{\rho_l}\left(p_v - 2\frac{\sigma}{R} - p_c\right)\right\}.$$

(2.57) $$\dot{T}_v = \frac{1}{B}\left\{-p_v y_R - \rho_v \frac{\partial \hat{h}_v}{\partial p_v}\cdot\left(1/\partial\rho_v/\partial p_v\right)\cdot\left[\frac{\dot{M}_{in}}{4\pi R^2} - \dot{M}_{vl} - \rho_v y_R\right] + - \frac{\dot{M}_{in}}{4\pi R^2}\left(\hat{h}_v - \hat{h}_i\right) + \dot{M}_{vl}\cdot\hat{h}_v - \dot{E}_{vl}\right\}.$$

(2.56) $$\dot{p}_v = \frac{3}{R\,\partial\rho_v/\partial p_v}\left\{\frac{\dot{M}_{in}}{4\pi R^2} - \dot{M}_{vl} - \rho_v y_R - \frac{R}{3}\frac{\partial\rho_v}{\partial T_v}\cdot\dot{T}_v\right\}.$$

(2.26) $$T_L = T_\infty - \left(\frac{D_l}{\pi}\right)^{1/2}\int_0^\tau \frac{(\partial T/\partial r)_R}{R^2(\tau-\zeta)^{1/2}}\cdot d\zeta .$$

(2.58) $$B = \frac{R}{3}\rho_v\left[\frac{\partial\hat{h}_v}{\partial T_v} - \left(\frac{\partial\hat{h}_v}{\partial p_v}\Big/\frac{\partial\rho_v}{\partial p_v}\right)\cdot\frac{\partial\rho_v}{\partial T_v}\right].$$

(2.27) $$\tau = \int_0^t R^4\cdot dt .$$

(2.34) $$\left(\frac{\partial T}{\partial r}\right)_R = -\frac{\dot{E}'_{vl}}{\kappa_l} .$$

(2.33) $$\dot{E}'_{vl} = \dot{M}_{co}\left(\hat{h}_v - \hat{h}_L^*\right) - \dot{M}_{ev}\cdot\hat{h}_{lv} .$$

(2.32) $$\dot{E}_{vl} = \dot{M}_{co}\cdot\hat{h}_v - \dot{M}_{ev}\cdot\hat{h}_L^* .$$

(2.29) $$\dot{M}_{vl} = \dot{M}_{co} - \dot{M}_{ev}$$

(2.30) $$\dot{M}_{co} = c_{co}\cdot\sqrt{\frac{M_w}{2\pi R_g}}\,\frac{p_v}{\sqrt{T_v}} .$$

(2.31) $$\dot{M}_{ev} = c_{ev}\cdot\sqrt{\frac{M_w}{2\pi R_g}}\,\frac{p_L^*(T_L)}{\sqrt{T_L}} .$$

(2.21) $$R' = \left(\frac{3}{4\pi}V_l + R^3\right)^{1/3} .$$

(2.23) $$R_c = \left(\frac{3}{4\pi}V_{c,0} + R_0'^3\right)^{1/3} ;$$ (2.37) $$n = \frac{c_{p,i}}{c_{v,i}}$$

(2.24) $$R_0' = \left(\frac{3}{4\pi}V_l + R_0^3\right)^{1/3} .$$

(2.22) $$p_c = p_{c,0}\left[\frac{1-(R_0'/R_c)^3}{1-(R'/R_c)^3}\right]^{\gamma_c} .$$

(2.39) $$\dot{M}_{in} = S\cdot\sqrt{\frac{p_i}{\hat{v}_i}\,n\left(\frac{2}{n+1}\right)^{\frac{n+1}{n-1}}} ; \quad p_v \le p_{crit} = p_i\left(\frac{2}{n+1}\right)^{\frac{n}{n-1}}$$

(2.41) $$\dot{M}_{in} = S\cdot\sqrt{2\frac{p_i}{\hat{v}_i}\frac{n}{n-1}\left[\left(\frac{p_v}{p_i}\right)^{2/n} - \left(\frac{p_v}{p_i}\right)^{\frac{n+1}{n}}\right]} ; \quad p_v > p_{crit}$$

3. Governing equations using the Theofanous approach.

3.1 Energy equation for the liquid

The equations of continuity for the liquid Eq.(2.2), of motion for the liquid Eq.(2.19) or Eq. (2.25), of mass transfer at the interface Eq. (2.29) to (2.31), of energy transfer at the interface Eq. (2.32) and (2.33)., the continuity equation for the vapor Eq. (2.46) and the energy equation for the vapor Eq. (2.53) remain unchanged.
Instead of using the approximate solution of Plesset-Zwick Eq. (2.26) the energy equation for the liquid is solved simultaneously with the other equations, although with some simplifications /3/.
The energy equation for a fluid in spherical coordinates and in presence of a spherical symmetry is:

$$\frac{\partial T}{\partial t} + u \frac{\partial T}{\partial r} = D_l \frac{1}{r^2} \frac{\partial}{\partial r} \left[r^2 \frac{\partial T}{\partial r} \right] . \tag{3.1}$$

Let us assume now that the temperature of the liquid is everywhere constant and equal to T_∞, except in a thermal boundary layer

$$R \leq r \leq R_L \tag{3.2}$$

near the phase interface

If we now consider the integral of Eq. (3.1) over the boundary layer, we obtain:

$$\int_R^{R_L} r^2 \frac{\partial T}{\partial t} dr + \int_R^{R_L} u r^2 \frac{\partial T}{\partial r} dr = \int_R^{R_L} D_l \frac{\partial}{\partial r} \left[r^2 \frac{\partial T}{\partial r} \right] dr . \tag{3.3}$$

Instead of solving (3.3) directly, the following approximate procedure is used: it is assumed that the temperature distribution in the liquid can be approached by a second-order distribution of the form

$$T(r) = ar^2 + br + c \quad ; \quad R \le r \le R_L \,. \tag{3.4}$$

$$T(r) = T_\infty \quad ; \quad r > R_L \,.$$

Now the coefficients, a,b,c, are determined using the following boundary conditions (see Fig. 2)

$$T(R) = T_L \,. \tag{3.5}$$

$$T(R_L) = T_\infty \,.$$

$$\left(\frac{\partial T}{\partial r}\right)_{R_L} = 0 \,.$$

Substituting Eq. (3.4) in (3.5) we get:

$$a = \frac{T_L - T_\infty}{(R_L - R)^2} \,. \tag{3.6}$$

$$b = -2\,\frac{(T_L - T_\infty)}{(R_L - R)^2} \cdot R_L \,.$$

$$c = T_\infty + \frac{(T_L - T_\infty)}{(R_L - R)^2} \cdot R_L^2 \,.$$

Substitution of (3.6) in (3.4) and rearrangement gives:

$$T(r) = T_\infty + (T_L - T_\infty)\left(\frac{R_L - r}{R_L - R}\right)^2 \quad ; \quad R \le r \le R_L . \tag{3.7}$$

$$T(r) = T_\infty \quad ; \quad r > R_L .$$

Using the temperature distribution Eq. (3.7) the various terms appearing in Eq. (3.3) are calculated:

$$\frac{\partial T}{\partial t} = \frac{\partial T_\infty}{\partial t} + \left(\frac{R_L - r}{R_L - R}\right)^2 \frac{\partial}{\partial t}(T_L - T_\infty) + 2(T_L - T_\infty)\frac{(R_L - R)(R_L - r)\dot{R}_L - (R_L - r)^2(\dot{R}_L - \dot{R})}{(R_L - R)^3} . \tag{3.8}$$

$$\frac{\partial T}{\partial r} = -2(T_L - T_\infty)\frac{R_L - r}{(R_L - R)^2} . \tag{3.9}$$

$$\frac{\partial}{\partial r}\left(r^2 \frac{\partial T}{\partial r}\right) = 2(T_L - T_\infty)\frac{3r^2 - 2R_L r}{(R_L - R)^2} . \tag{3.10}$$

We consider for simplicity the case:

$$T_\infty = \text{const.} \tag{3.11}$$

and substitute the expressions (3.8) to (3.10) in Eq. (3.3), using also the continuity equation for the liquid in the form (2.6), and get:

$$\frac{1}{(R_L - R)^2}\frac{\partial T_L}{\partial t}\int_R^{R_L} r^2 (R_L - \;)^2 dr + 2\frac{(T_L - T_\infty)}{(R_L - R)^2}\dot{R}_L \int_R^{R_L} r^2 (R_L - r)\, dr + \tag{3.12}$$

$$-2\frac{T_L - T_\infty}{(R_L - R)^3}(\dot{R}_L - \dot{R})\int_R^{R_L} r^2 (R_L - r)^3 dr - 2\frac{T_L - T_\infty}{(R_L - R)^2} R^2 \dot{R} \int_R^{R_L} (R_L - r)\, dr =$$

$$= 2D_l \frac{T_L - T_\infty}{(R_L - R)^2}\int_R^{R_L} (3R^2 - 2R_L r)\, dr .$$

Performing the integration and after some rearrangement one gets:

$$(3.13)\quad (R_L-R)\left(R_L^2+3R_LR+6R^2\right)\frac{dT_L}{dt}+(T_L-T_\infty)\left(3R_L^2+4R_LR+3R^2\right)\frac{dR_L}{dt}+$$
$$+2(T_L-T_\infty)\left(R_L^2+3R_LR-9R^2\right)\frac{dR}{dt}=60\,D_\ell\,(T_L-T_\infty)\frac{R^2}{(R_L-R)}\,.$$

At this point we perform a change of variable, intoducing the boundary layer thickness:

$$(3.14)\quad \delta = R_L - R$$

and Eq.(3.13) becomes finally:

$$(3.15)\quad \delta\left(10R^2+5R\delta+\delta^2\right)\frac{dT_L}{dt}+(T_L-T_\infty)\left(20R\delta+5\delta^2\right)\frac{dR}{dt}+$$
$$+(T_L-T_\infty)\left(10R^2+10R\delta+3\delta^2\right)\frac{d\delta}{dt}=60\,D_\ell\,(T_L-T_\infty)\frac{R^2}{\delta}\,.$$

3.2 Equation of energy transfer at the interface

In order to couple the heat diffusion problem in the liquid with the interphase energy transfer, Eq. (2.34) is used as a boundary condition for the energy equation for the liquid.
Substituting the postulated temperature distribution Eq.(3.7) in Eq. (2.34), using also Eq. (3.9) and (3.14) one has:

$$(3.16)\quad -2\,\frac{T_L-T_\infty}{\delta}=-\frac{\dot{E}'_{v\ell}}{K_\ell}$$

Now we differentiate Eq. (3.16) with respect to time assuming for simplicity

(3.17) $$K_l = \text{const.}$$

and, using also Eq. (2.33), (2.30), (2.31) (3.11), we obtain:

(3.18) $$-\frac{T_L - T_\infty}{\delta^2}\dot{\delta} - \frac{1}{2K_l}\dot{M}_{c\sigma}\left[\frac{\partial \hat{h}_v}{\partial p_v} + \frac{(\hat{h}_v - \hat{h}_L^*)}{p_v}\right]\cdot \dot{p}_v +$$
$$+\frac{1}{2K_l}\dot{M}_{c\sigma}\cdot\left[-\frac{\partial \hat{h}_v}{\partial T_v} + \frac{(\hat{h}_v - h_L^*)}{2T_v}\right]\dot{T}_v +$$
$$+\left\{\frac{1}{\delta} + \frac{1}{2K_l}\left[\dot{M}_{c\sigma}\frac{d\hat{h}_L^*}{dT_L} + \dot{M}_{ev}\left(\frac{d\hat{h}_{lv}}{dT_L} + \frac{\hat{h}_{lv}}{p_L^*}\frac{dp_L^*}{dT_L} - \frac{\hat{h}_{lv}}{2T_L}\right)\right]\right\}\dot{T}_L = 0.$$

3.3 Final form of the differential equations

The problem of the bubble growth is completely described by the following equations:

a) Equation of the motion for the liquid, Eq. (2.25)
b) Continuity equation for the vapor, Eq. (2.46)
c) Energy equation for the vapor, Eq. (2.53)
d) Energy equation for the liquid, Eq. (3.15)
e) Equation of energy transfer at the interface, Eq. (3.18)

Equations a), b), c) are treated exactly the same way as in § 2.9 obtaining Equations (2.54), (2.55), (2.56), (2.57) and (2.58). Then we use Eq. (3.15) and (2.54) to obtain:

(3.19) $$\dot{T}_L = \frac{(T_L - T_\infty)}{\delta(10R^2 + 5R\delta + \delta^2)}\left[-(20R\delta + 5\delta^2)y_R + \right.$$
$$\left. -(10R^2 + 10R\delta + 3\delta^2)\dot{\delta} + 60D_l\frac{R^2}{\delta}\right].$$

Substituting Eq. (3.19) in Eq. (3.18) and solving for $\dot{\delta}$ one gets finally:

$$\dot{\delta} = \frac{1}{C}\left\{\frac{1}{2K_e}\dot{M}_{cv}\left[\frac{\partial \hat{h}_v}{\partial p_v} + \frac{(\hat{h}_v - \hat{h}_L^*)}{p_v}\right]\dot{p}_v + \right.$$

$$-\frac{1}{2K_e}\dot{M}_{cv}\left[-\frac{\partial \hat{h}_v}{\partial T_v} + \frac{(\hat{h}_v - \hat{h}_L^*)}{2T_v}\right]\dot{T}_v +$$

$$\left. - A\,\frac{(T_L - T_\infty)}{\delta(10R^2 + 5R\delta + \delta^2)}\left[-(20R\delta + 5\delta^2)\,y_R + 60 D_\ell \frac{R^2}{\delta}\right]\right\}. \tag{3.20}$$

where

$$C = -\frac{T_L - T_\infty}{\delta}\left[\frac{1}{\delta} + A\,\frac{(10R^2 + 10R\delta + 3\delta^2)}{(10R^2 + 5R\delta + \delta^2)}\right]. \tag{3.21}$$

$$A = \frac{1}{\delta} + \frac{1}{2K_e}\left[\dot{M}_{cv}\frac{d\hat{h}_L^*}{dT_L} + \dot{M}_{ev}\left(\frac{d\hat{h}_{\ell v}}{dT_L} + \frac{\hat{h}_{\ell v}}{p_L^*}\frac{dp_L^*}{dT_L} - \frac{\hat{h}_{\ell v}}{2T_L}\right)\right]. \tag{3.22}$$

Equations (2-54), (2.55), (2.57), (2.56), (3.20), (3.19) form the system of six differential equations in the six unknown functions R, Y_R, T_v, p_v, δ, T_L, which has to be solved. In Table 2 all the equations and the formulae necessary for the solution of the problem are listed.

Table 2

Summary of the governing equations using the Theofanous solution

(2.54) $$\dot{R} = y_R$$

(2.55) $$\dot{y}_R = \frac{R'}{R(R'-R)} \left\{ -\frac{1}{2}\left[3 - 4\frac{R}{R'} + \left(\frac{R}{R'}\right)^4\right] \cdot y_R^2 + \right.$$
$$\left. - \left[4\frac{\mu_\ell}{\rho_\ell}\left(\frac{1}{R} - \frac{R^2}{R'^3}\right)\right] y_R + \frac{1}{\rho_\ell}\left(p_v - 2\frac{\sigma}{R} - p_c\right) \right\}.$$

(2.57) $$\dot{T}_v = \frac{1}{B}\left\{ -p_v y_R - \rho_v \frac{\partial \hat{h}_v}{\partial p_v}\left(1/\partial\rho_v/\partial p_v\right)\cdot\left[\frac{\dot{M}_{in}}{4\pi R^2} - \dot{M}_{ve} - \rho_v y_R\right] + \right.$$
$$\left. - \frac{\dot{M}_{in}}{4\pi R^2}\left(\hat{h}_v - \hat{h}_i\right) + \dot{M}_{ve}\cdot\hat{h}_v - \dot{E}_{ve} \right\}.$$

(2.56) $$\dot{p}_v = \frac{3}{R(\partial\rho_v/\partial p_v)}\left\{ \frac{\dot{M}_{in}}{4\pi R^2} - \dot{M}_{ve} - \rho_v y_R - \frac{R}{3}\frac{\partial \rho_v}{\partial T_v}\dot{T}_v \right\}.$$

(3.20) $$\dot{\delta} = \frac{1}{C}\left\{ \frac{1}{2k_\ell}\dot{M}_{co}\left[\frac{\partial \hat{h}_v}{\partial p_v} + \frac{(\hat{h}_v - \hat{h}_L^*)}{p_v}\right]\dot{p}_v - \frac{1}{2k_\ell}\dot{M}_{co}\left[-\frac{\partial \hat{h}_v}{\partial T_v} + \frac{(\hat{h}_v - \hat{h}_L^*)}{2T_v}\right]\dot{T}_v + \right.$$
$$\left. - A\frac{(T_L - T_\infty)}{\delta(10R^2 + 5R\delta + \delta^2)}\left[-(20R\delta + 5\delta^2)y_R + 60 D_\ell \frac{R^2}{\delta}\right] \right\}.$$

(3.19) $$\dot{T}_L = \frac{(T_L - T_\infty)}{\delta(10R^2 + 5R\delta + \delta^2)}\left[-(20R\delta + 5\delta^2)y_R - (10R^2 + 10R\delta + 3\delta^2)\dot{\delta} + \right.$$
$$\left. + 60 D_\ell \frac{R^2}{\delta}\right].$$

(2.58) $$B = \frac{R}{3}\rho_v\left[\frac{\partial \hat{h}_v}{\partial T_v} - \left(\frac{\partial \hat{h}_v}{\partial p_v}\Big/\frac{\partial \rho_v}{\partial p_v}\right)\frac{\partial \rho_v}{\partial T_v}\right].$$

(3.21) $$C = -\frac{(T_L - T_\infty)}{\delta}\left[\frac{1}{\delta} + A\frac{(10R^2 + 10R\delta + 3\delta^2)}{(10R^2 + 5R\delta + \delta^2)}\right].$$

(3.22) $$A = \frac{1}{\delta} + \frac{1}{2k_\ell}\left[\dot{M}_{co}\frac{d\hat{h}_L^*}{dT_L} + \dot{M}_{ev}\left(\frac{d\hat{h}_{\ell v}}{dT_L} + \frac{\hat{h}_{\ell v}}{p_L^*}\frac{dp_L^*}{dT_L} - \frac{\hat{h}_{\ell v}}{2T_L}\right)\right].$$

(2.32) $$\dot{E}_{ve} = \dot{M}_{co}\hat{h}_v - \dot{M}_{ev}\hat{h}_L^*.$$

(2.29) $$\dot{M}_{ve} = \dot{M}_{co} - \dot{M}_{ev}$$

(2.30) $$\dot{M}_{co} = c_{co}\sqrt{\frac{M_w}{2\pi R_g}}\frac{p_v}{\sqrt{T_v}}.$$

(2.31) $$\dot{M}_{ev} = c_{ev}\sqrt{\frac{M_w}{2\pi R_g}}\frac{p_L^*}{\sqrt{T_L}}.$$

(2.21) $$R' = \left(\frac{3}{4\pi}V_\ell + R^3\right)^{1/3}.$$

(2.23) $$R_c = \left(\frac{3}{4\pi}V_{c,0} + R_0'^3\right)^{1/3}.$$;

(2.37) $$n = \frac{c_{p,i}}{c_{v,i}}.$$

(2.24) $$R_0' = \left(\frac{3}{4\pi}V_\ell + R_0^3\right)^{1/3}.$$

(2.22) $$p_c = p_{c,0}\cdot\left[\frac{1 - (R_0'/R_c)^3}{1 - (R_0/R_c)^3}\right]^{\gamma_c}.$$

(2.39) $$\dot{M}_{in} = S\cdot\sqrt{\frac{p_i}{\vartheta_i}n\left(\frac{2}{n+1}\right)^{(n+1)/(n-1)}}$$; $p_v \le p_{crit} = p_i\left(\frac{2}{n+1}\right)^{n/(n-1)}$

(2.41) $$\dot{M}_{in} = S\cdot\sqrt{2\frac{p_i}{\vartheta_i}\frac{n}{n-1}\left[\left(\frac{p_v}{p_i}\right)^{2/n} - \left(\frac{p_v}{p_i}\right)^{(n+1)/n}\right]}$$; $p_v > p_{crit}$.

4. Numerical solution of the differential equations obtained using the Plesset-Zwick formulae

4.1 Method of numerical solution

The numerical method used to solve the system of differential equations is a predictor-corrector method /6/.
The formula used for the predictor is:

$$y_{m+1}^{(0)} = y_{m-1} + 2h\, f(x_m, y_m) . \tag{4.1}$$

while the corrector formula is

$$y_{m+1}^{(i)} = y_m + \frac{h}{2}\left[f(x_m, y_m) + f\left(x_{m+1}, y_{m+1}^{(i-1)}\right)\right] . \tag{4.2}$$

where f represents the derivative with respect to x of the generic unknown function y(x), and h is the time step defined by

$$h = x_{m+1} - x_m = x_m - x_{m-1} . \tag{4.3}$$

When the solution $y_{m+1}^{(i)}$ has been obtained with the desired accuracy, the following final correction is applied, providing more accuracy /6/

$$y_{m+1} = y_{m+1}^{(i)} + \frac{1}{5}\left(y_{m+1}^{(0)} - y_{m+1}^{(i)}\right) . \tag{4.4}$$

In order to start the solution and to be able to change the time step by either doubling or having it during the solution, use of a self-starting Runge-Kutta fourth order procedure is made /6/ :

$$y_{m+1} = y_m + \frac{h}{6}\left(K_1 + K_2 + K_3 + K_4\right) . \tag{4.5}$$

where

$$K_1 = f(x_m, y_m).$$

$$K_2 = f\left(x_m + \frac{h}{2}, y_m + K_1 \frac{h}{2}\right). \tag{4.6}$$

$$K_3 = f\left(x_m + \frac{h}{2}, y_m + K_2 \frac{h}{2}\right).$$

$$K_4 = f\left(x_m + h, y_m + K_3 h\right).$$

4.2 Use of the Plesset-Zwick formula

The Plesset-Zwick formula (2.26) is solved iteratively at each step of the numerical integration. An iterative solution is necessary since the integral appearing at the right hand side is a function of $T_L(t)$. Starting values for the iterative procedure are calculated by second order or first order interpolation formulae using values of T_L at the preceding time steps.

A difficulty arises in the numerical calculation of the integral appearing in (2.26), because the integral becomes infinite at the right boundary of the domain of integration. An approximated solution is obtained by replacing the curve

$$F(\zeta) = \frac{(\partial T/\partial z)_R(\zeta)}{R^2(\zeta)} . \tag{4.7}$$

by a second order curve $\bar{F}(\zeta)$ fitting the values of $F(\zeta)$ at the last three points of the integration domain, ζ'', ζ' and τ respectively (see Fig. 3)

$$\bar{F}(\zeta) = c_1 \zeta^2 + c_2 \zeta + c_3 \; ; \; \zeta'' \le \zeta \le \tau . \tag{4.8}$$

where

$$c_1 = \frac{1}{\tau - \zeta'} \left[\frac{F(\tau) - F(\zeta'')}{\tau - \zeta''} - \frac{F(\zeta') - F(\zeta'')}{\zeta' - \zeta''} \right].$$

$$c_2 = -(\zeta' - \zeta'') c_1 + \frac{F(\zeta') - F(\zeta'')}{\zeta' - \zeta''} . \tag{4.9}$$

$$c_3 = -\zeta''^2 \cdot c_1 - \zeta'' c_2 + F(\zeta'').$$

By integrating (4.7) one gets:

$$(4.10)\qquad I_{Last} = \int_{z''}^{\tau} \frac{F(z)}{(\tau - z)^{1/2}}\, dz = 2\left\{\left[\tau^2 - \frac{2}{3}\tau(\tau - z') + \frac{1}{5}(\tau - z')^2\right]c_1 + \left[\tau - \frac{1}{3}(\tau - z')\right]\cdot c_2 + c_3\right\}\cdot\sqrt{\tau - z'}\,.$$

At the beginning of the solution, when only two points are available, a first-order approach is used:

$$(4.11)\qquad \bar{F}(z) = F(z') + \frac{F(\tau) - F(z')}{\tau - z'}(z - z')\,;\quad z' \le z \le \tau\,.$$

and the approximated solution is

$$(4.12)\qquad I_{Last} = \frac{2}{3}\sqrt{(\tau - z')}\cdot\left[F(z') + 2F(\tau)\right].$$

For the numerical evaluation of the integrals appearing in (2.27) and (2.26), the functions to be integrated, which are known only at certain points, are replaced by second order or first order fittings and then analytically integrated. Since the time step is variable, the distance between the points where the functions are known is not constant, and more accurate integration formulae like Gauss formulae can not be used.

4.3 Derivatives of the physical properties

The derivatives of the physical properties appearing in the formulae of Table 1 are computed using the formula /7/

$$(4.13)\qquad F'(i) = \frac{F(i+1) - F(i-1)}{2h}\,.$$

4.4 Vapor source treatment

In order to improve the rapidity of convergence of the solution, the equation (2.41) is replaced by the linearized formula

$$\dot{M}_{in} = S \cdot \dot{M}_{lin} \cdot \left[1 - \frac{p_v - p_{lin}}{p_i - p_{lin}} \right] . \tag{4.14}$$

in the domain

$$p_{lin} \leq p_v \leq p_i \quad . \tag{4.15}$$

where

$$p_{lin} = p_{crit} + 0.9 \left(p_i - p_{crit} \right) . \tag{4.16}$$

The cross section S of the orifice is varied according to Fig. 4 and the value S_{max} is computed in order to give a certain chosen value $\dot{M}_{in,\,crit}$ of the mass flow rate.

4.5 Initial conditions and values of the parameters

We present solutions of the set of equations listed in Table 1, obtained with the initial conditions listed in Table 3:

Table 3 Initial Conditions

(4.17) $R(o) = 0.1$ m

(4.18) $Y_R(o) = 0$ m/sec

(4.19) $p_v(o) = 1.013 \times 10^5$ N/m^2

(4.20) $T_v(o) = T_v^* \left[p_v(o)\right] = 1154.59$K

(4.21) $T_L(o) = 800$K

The bubble is supposed to contain saturated vapor at atmospheric pressure. The temperature in the liquid is initially uniform and equal to the temperature at infinity. The initial conditions are non-equilibrium conditions because the vapor temperature is different from the liquid interface temperature.

In Table 4 the values assigned to the most important parameters in the solutions are shown.

Table 4

Values of the parameters:

T_i = 1700K
p_i = $5. \times 10^5$ N/m^2
R_g = 8314. J/mol·K
M_W = 23. kg/mol
μ_l = 0.227×10^{-3} kg/m·sec
ρ_l = 825.8 kg/m^3
σ = 0.154 N/m
$c_{p,l}$ = 1259.7 J/ kg·K
K_l = 65.6 J/sec·m·K
T_∞ = 800K
p_∞ = $p_{v,o} - 2 \frac{\sigma}{R_o}$
v_l = 110 m^3
$v_{c,o}$ = 70 m^3
$p_{c,o}$ = p_∞
γ_c = 1.667

The orifice connecting the bubble with the source starts to open linearly at time t=0 and is completely open after 1 msec. Orifice parameters are so chosen that a maximum mass rate from the core to the bubble of 100 kg/sec of hot sodium vapor is reached.

To compute the physical properties of sodium such as enthalpies, saturation pressure etc, use has been made of MAPLIB-routines /8, 10/

5. Results

The results of three different solutions of the set of equations obtained with the Plesset-Zwick approach (Table 1) are presented, for the cases:

a) $c = c_{ev} = c_{co} = 0.1$

b) $c = c_{ev} = c_{co} = 0.01$

c) $c = c_{ev} = c_{co} = 1.$

The initial conditions and the values of the other parameters were exactly the same in the three cases presented, and have been listed in Table 3 and Table 4 respectively.
Figures 5 to 14 show a comparison of the results of the three cases in the first 270 msec.

A decrease in the value of the coefficients c, as it would be in presence of noncondensable gases which tend to accumulate near the bubble wall, causes a slight increase of the growth velocity and a much greater increase of the vapor temperature, as expected. The liquid interface temperature, on the other hand, is much decreased .

Figures 15 to 24 show the same curves in the initial region (about $o \div 3$ msec).

The calculations for cases a) and b) have been extended up to 1.5sec and 2.4 sec, respectively.
Figures 25 to 29 show the results for case a) and Figures 30 to 34 show the results for case b).

Oscillations are mainly due to the presence of the cover gas volume.

In Table 5 some results are listed for the three cases presented. The values of the maximum radius, growth velocity, vapor temperature, vapor pressure, liquid interface temperature and introduced mass flow rate are given for the first threee oscillations of the bubble.

For the case c=1 only the first oscillation is given. In the same Table the values of T_v, p_v, T_L at the time when the maximum radius (at the first oscillation) is reached, are also given.
In general the difference between the results of case c=0.1 and case c=0.01 is greater than the difference between case c=1. and case c=0.1. Particularly interesting is to compare the values at the first maximum radius: going from case c=1. to case c=0.01 the maximum bubble radius at the first oscillation increases by 9.0%, the time is 9.5% smaller, the vapor temperature increases by 9.6%, the vapor pressure increases by 31.6% and the liquid interface temperature decreases by 19.3%.
The maximum growth velocity at the first oscillation increases by 1.6% from the case c=1. to case c=0.01.
In Table 5 the values of the total transferred masses, M_{in}, M_{co}, M_{ev} and energies E_{v1}, E_{v1}' at the time when the radius reaches its maximum value (first oscillation) are also given.
From case c=1 to case c=0.01, M_{in} decreases by 8.2%, E_{v1} decreases by 64%, E_{v1}' decreases by 63% and M_{co} and M_{ev} are reduced to 1.3% and 0.07% of the value at c=1., respectively.

Table 5 Results of Calculations

	C = 1.		C = 0.1		C = 0.01	
	value	time (ms)	value	time (ms)	value	time (ms)
$R_{max,1}$ (m)	1.828	151.	1.861	152.	1.993	143.
$R_{max,2}$ "	(-)	(-)	2.068	337.	2.108	311.
$R_{max,3}$ "	(-)	(-)	2.136	492.	2.156	442.
$Y_{R,max}$ 1 (m/s)	18.71	22.0	18.76	22.4	19.00	243.
2 "	(-)	(-)	8.68	290.	7.70	259.
3 "	(-)	(-)	7.60	454.	6.75	409.
$T_{v,max}$ 1 (^{o}K)	1502.	0.30	1598.	0.63	1572.	0.48
2 "	1307.	247.	1372.	230.	1627.	220.
3 "	(-)	(-)	1376.	408.	1612.	371.
$P_{v,max}$ 1 (Pa)	4.98×10^5	1.14	4.98×10^5	1.03	5.00×10^5	0.99
2 "	3.34×10^5	248.	3.31×10^5	244.	3.74×10^5	227.
3 "	(-)	(-)	3.81×10^5	415.	4.15×10^5	371.
$T_{L,max}$ 1 (^{o}K)	1354.	2.67	1293.	18.8	963.	32.8
2 "	(-)	(-)	1290.	244.	1121.	246.
3 "	(-)	(-)	1314.	415.	1195.	382.
$\dot{M}_{in,max}$ 1 (kg/s)	24	0.26	19.	0.2	18.	0.2
2 "	(-)	(-)	100.	44.	100.	64.
3 "	(-)	(-)	(-)	(-)	(-)	(-)
$\int \dot{M}_{in}$ at $R=R_{max,1}$ (kg)	13.21	151.	13.27	152.	12.12	143.
$\int \dot{M}_{co}$ at $R=R_{max,1}$ (kg)	231.		24.4		2.92	
$\int \dot{M}_{ev}$ at $R=R_{max,1}$ (kg)	224.		17.5		0.16	

continued (tab. 5)

$\int \dot{E}_{v1}$ at $R=R_{max,1}$ (J)	3.86×10^7		3.73×10^7		1.39×10^7	
$\int \dot{E}'_{v1}$ at $R=R_{max,1}$ (J)	3.21×10^7		3.06×10^7		1.20×10^7	
T_v at $R=R_{max,1}$ (K)	1154.00	151.	1235.	152.	1265.	143.
P_v at $R=R_{max,1}$ (Pa)	0.919×10^5		0.986×10^5		1.209×10^5	
T_L at $R=R_{max,1}$ (K)	1141.		1117.		920.	

Acknowledgement

The author wishes to thank Dr. M. Dalle Donne, who suggested the work, for the advice and the helpful discussions.

References

/1/ M.S. Plesset, S.A. Zwick
A Nonsteady Heat Diffusion Problem with Spherical Symmetry,
J. Appl. Phys. 23, 95-98 (1952)

/2/ R.W. Schrage
A Theoretical Study of Interphase Mass Transfer,
Columbia University Press, New York (1953)

/3/ T. Theofanous, L. Biasi, H.S. Isbin, H. Fauske
A Theoretical Study on Bubble Growth in Constant and Time-dependent Pressure Fields, Chem. Eng. Sci. 24 (3), 885-897 (1969)

/4/ A.B. Reynolds and G. Berthoud
Expansion and Collapse of Large Two-Phase Bubbles
99th ASME Wint. Ann. Mtg. (1978), Proceedings

/5/ A.J. Brook and D.S. Mills
NABUB: a non-saturated model of coolant boiling in a fast reactor sub-assembly, TRG Report 2733(R), UKAEA (1975)

/6/ D.D. Mc Craken, W.S. Dorn
Numerical Methods and FORTRAN Programming
J.Wiley and Sons (1964).

/7/ J.M.Mc. Cormick, M.G. Salvadori,
Numerical Methods in FORTRAN
Prentice Hall (1964)

/8/ U. Schumann
MAPLIB:Ein Programmsystem zur Bereitstellung von Stoffdaten für Rechenprogramme : KfK-Bericht Nr. 1253 (1970)

/9/ S. Goldstein (ed)
Modern Developments in Fluid Dynamics , Vol 1. Clarendon Press, Oxford (1952).

/10/ R. Schuster, W. Zimmerer
Darstellung der Stoffdaten des Systems MAPLIB in tabellarischer und graphischer Form, KfK-Ext. Bericht 8/77-1 (1977)

/11/ M.S. Plesset and S.A. Zwick
The Growth of Vapor Bubbles in Superheated Liquids
J. Appl. Phys. 25, 493-500 (1954)

/12/ S.A. Zwick and M.S. Plesset
On the Dynamics of Small Vapor Bubbles in Liquids
J. Math. Phys. 33, 308-330 (1955)

/13/ W.J. Bornhorst, G.N. Hatsopoulos
Bubble-Growth Calculation without Neglect of Interfacial Discontinuities, Trans. of the A.S.M.E. 34, Series E,4 847-853 (1967)

/14/ W.J. Bornhorst, G.N. Hatsopoulos
Analysis of a Liquid Vapor Phase Change by the Methods of Irreversible Thermodynamics; Trans.of the A.S.M.E. 34, Series E,4, 840-846 (1967)

/15/ G. Birkhoff, R.S. Margulies and W.A. Horning
Spherical Bubble Growth, Physics Fluids 1 , 201-204 (1958)

/16/ M.Dalle Donne, and M.P. Ferranti
The growth of vapor bubbles in superheated sodium; Int. J. Heat Mass Transfer 18, 477-493 (1975)

/17/ A. Prosperetti. M.S. Plesset,
Vapor Bubble Growth in a Superheated Liquid
J. Fluid Mech. 85, 349-368 (1978).

/18/ A.B. Reynolds, M.F. Kennedy, H. Honig
Condensation of a Large Sodium Vapor Bubble after a Fast Reactor Disassembly Accident, Trans. Am. Nucl. Soc. 14, 738-739 (1971)

/19/ T.G. Theofanous , H.K. Fauske
The Effect of Noncondensables on the Rate of Sodium Vapor Condensation from a Single-Rising HCDA Bubble; Nucl. Techn.19 132-139 (1973)

/20/ M.N. Özişik, T.S. Kress,
Effects of Internal Circulation Velocity and Noncondensable Gas on Vapor Condensation from a Rising Bubble; Nucl. Sci. and Engn. 66, 397-405 (1978)

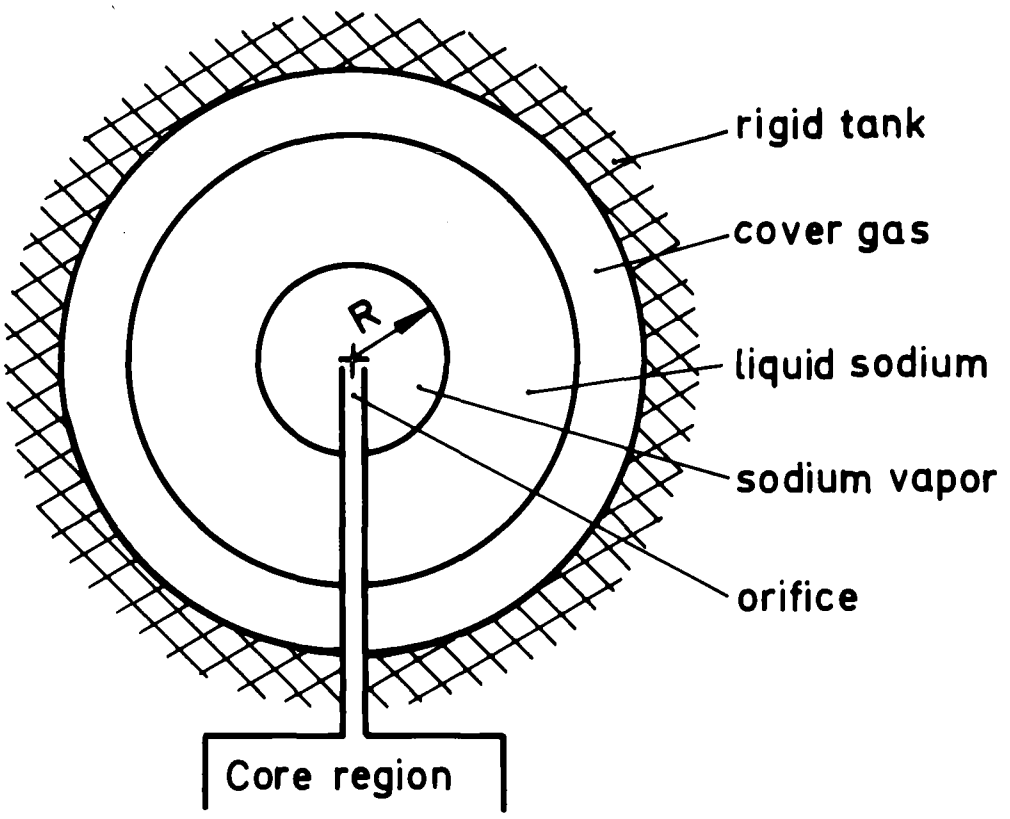

Fig.1: Schematic representation of the used model

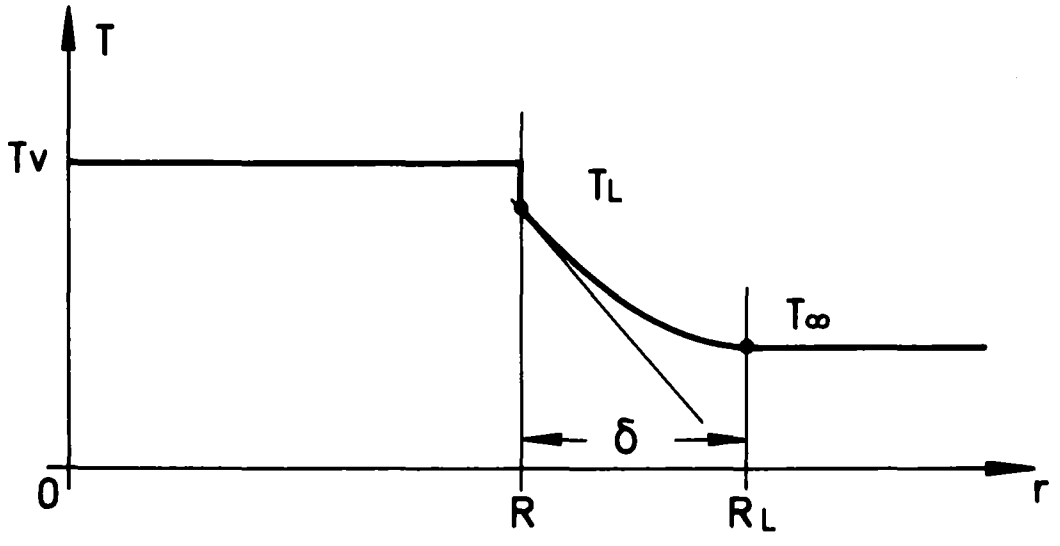

Fig.2: Temperature distribution in the Theofanous approach

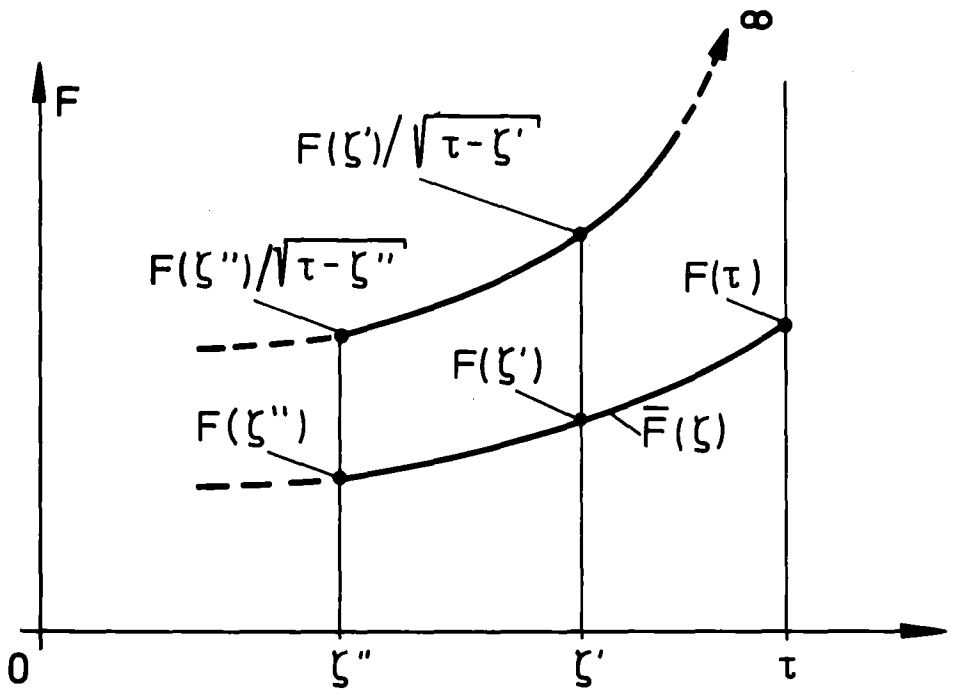

Fig.3: Integration of the Plesset-Zwick equation over the last interval

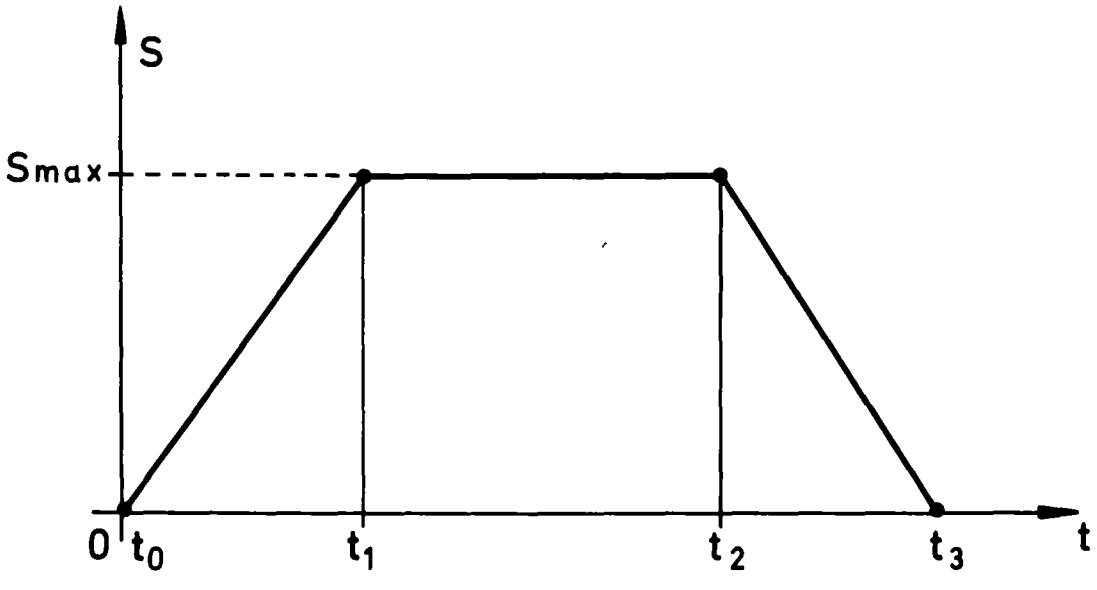

Fig. 4: Variation of the orifice cross section

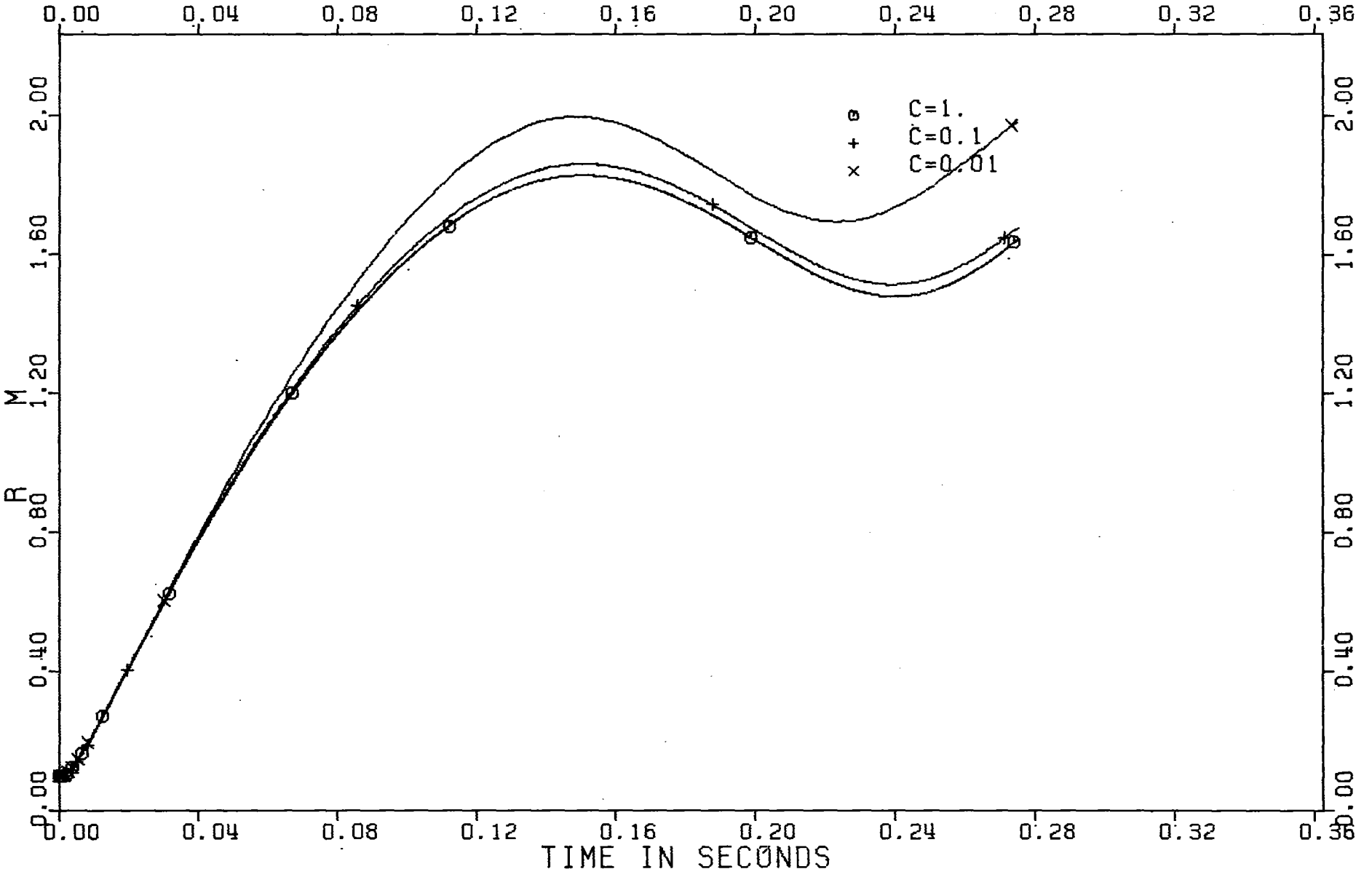

Fig. 5 : Comparison of results : bubble radius R

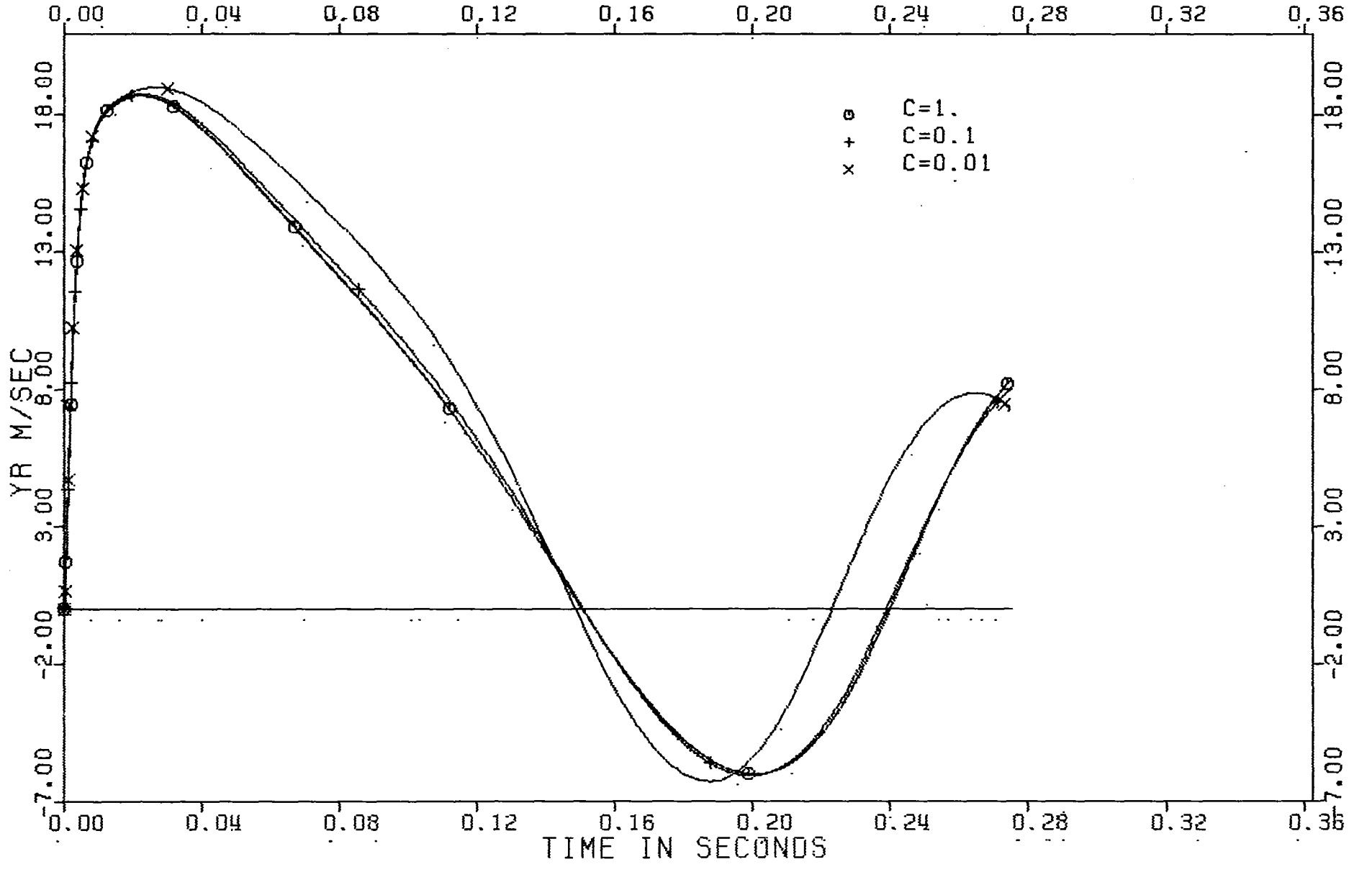

Fig. 6 : Comparison of results : bubble growth velocity Y_R

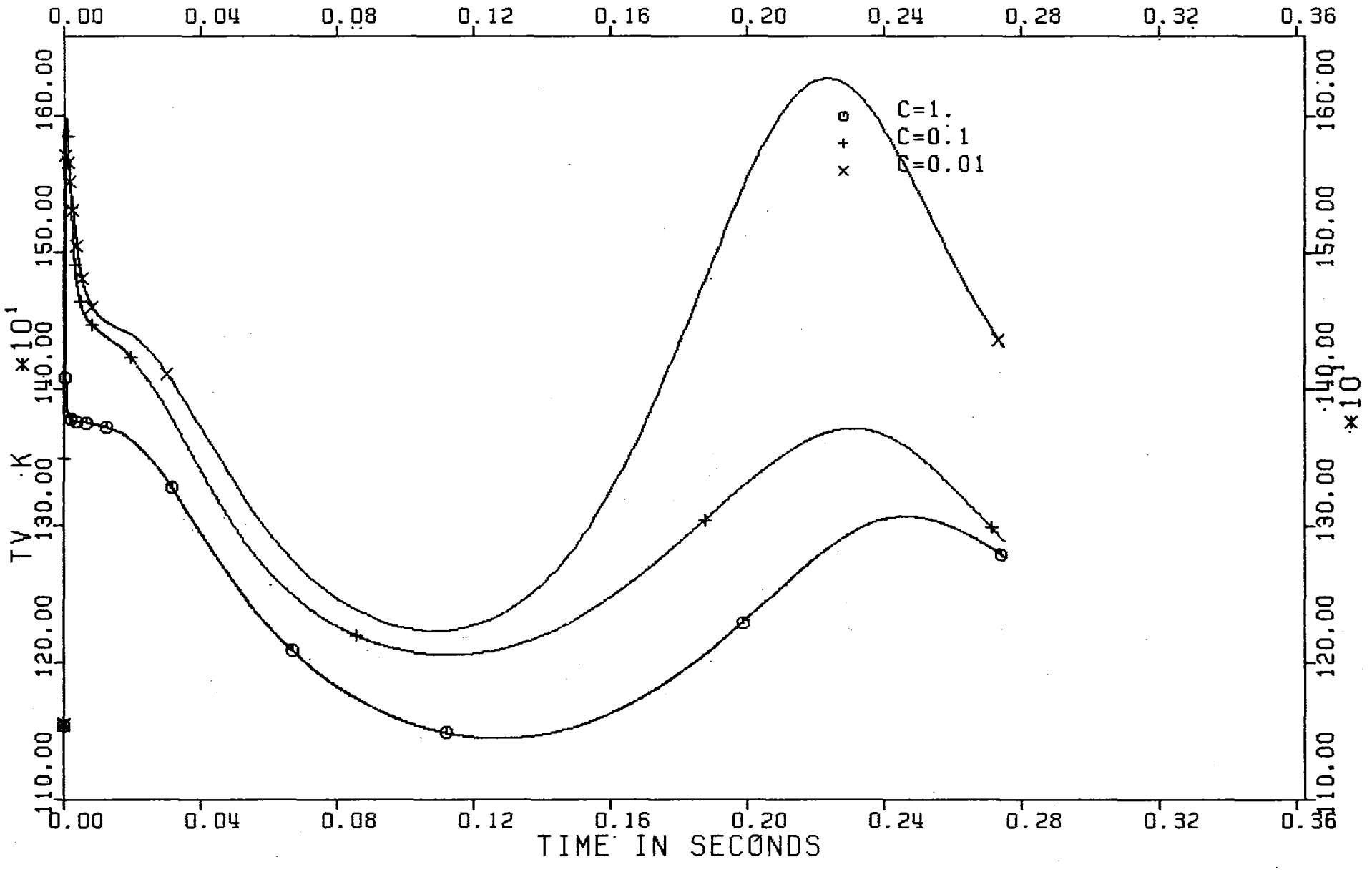

Fig. 7 : Comparison of results : bubble vapor temperature T_v

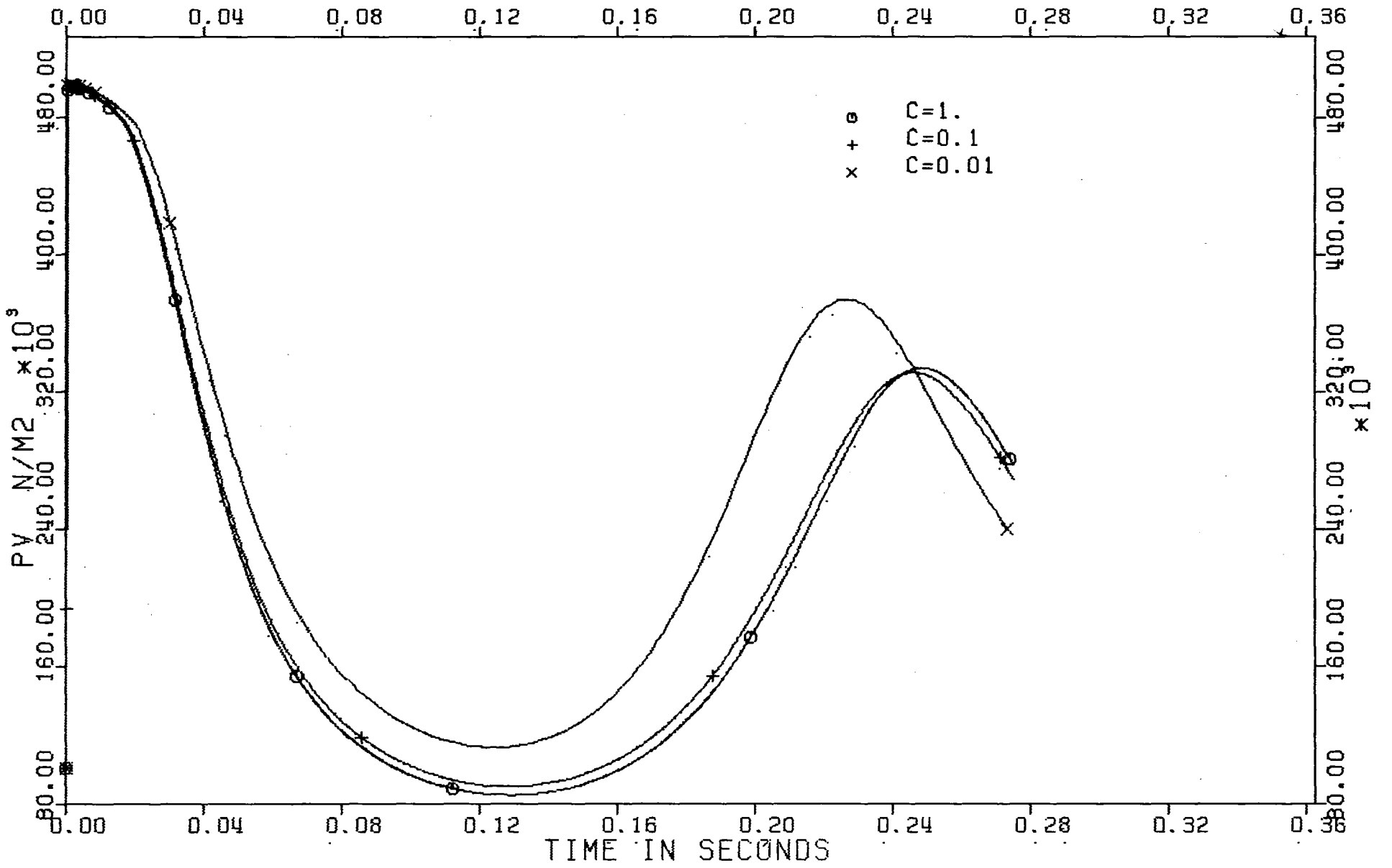

Fig. 8 : Comparison of results : bubble pressure p_v

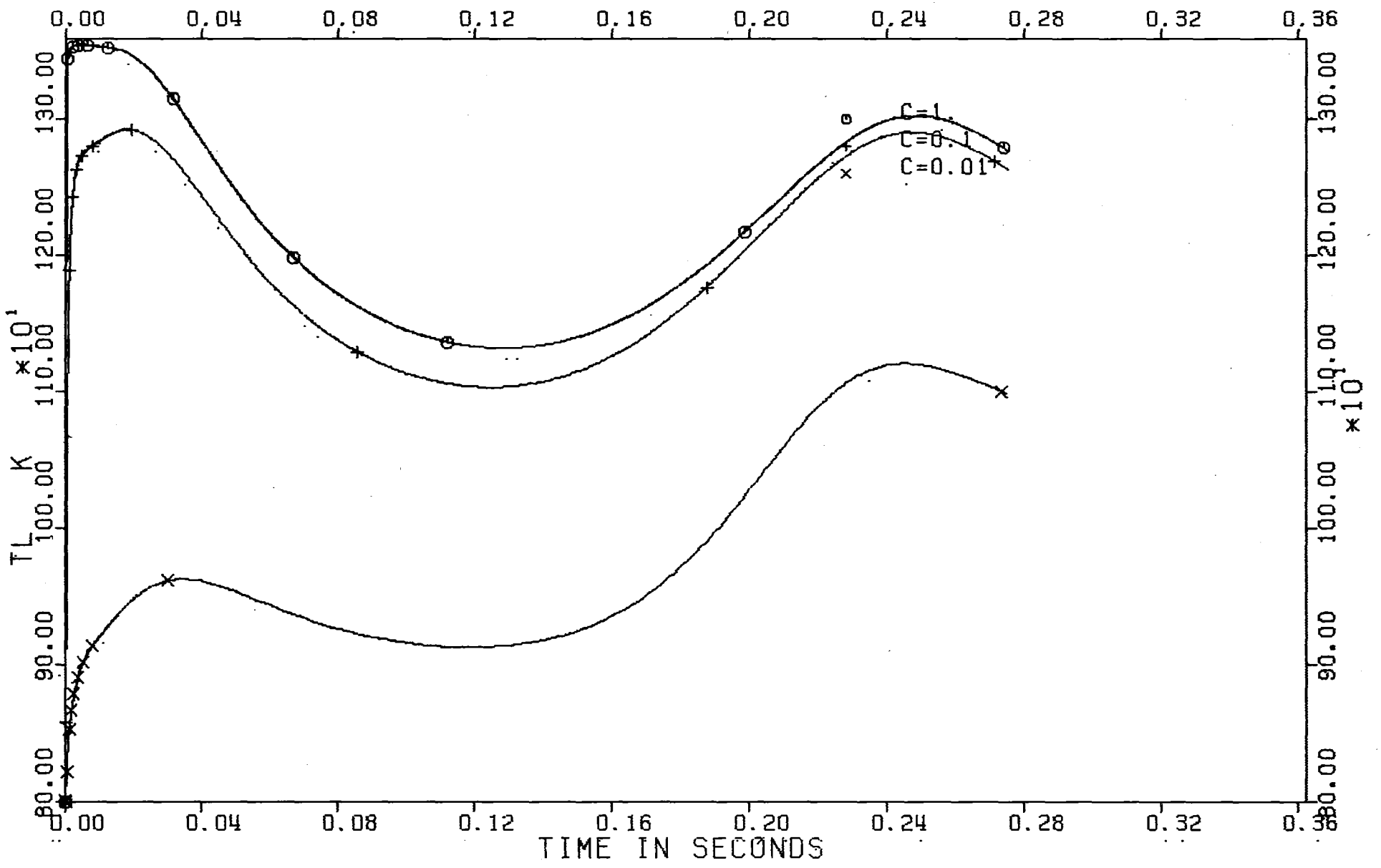

Fig. 9 : Comparison of results : liquid interface temperature T_L

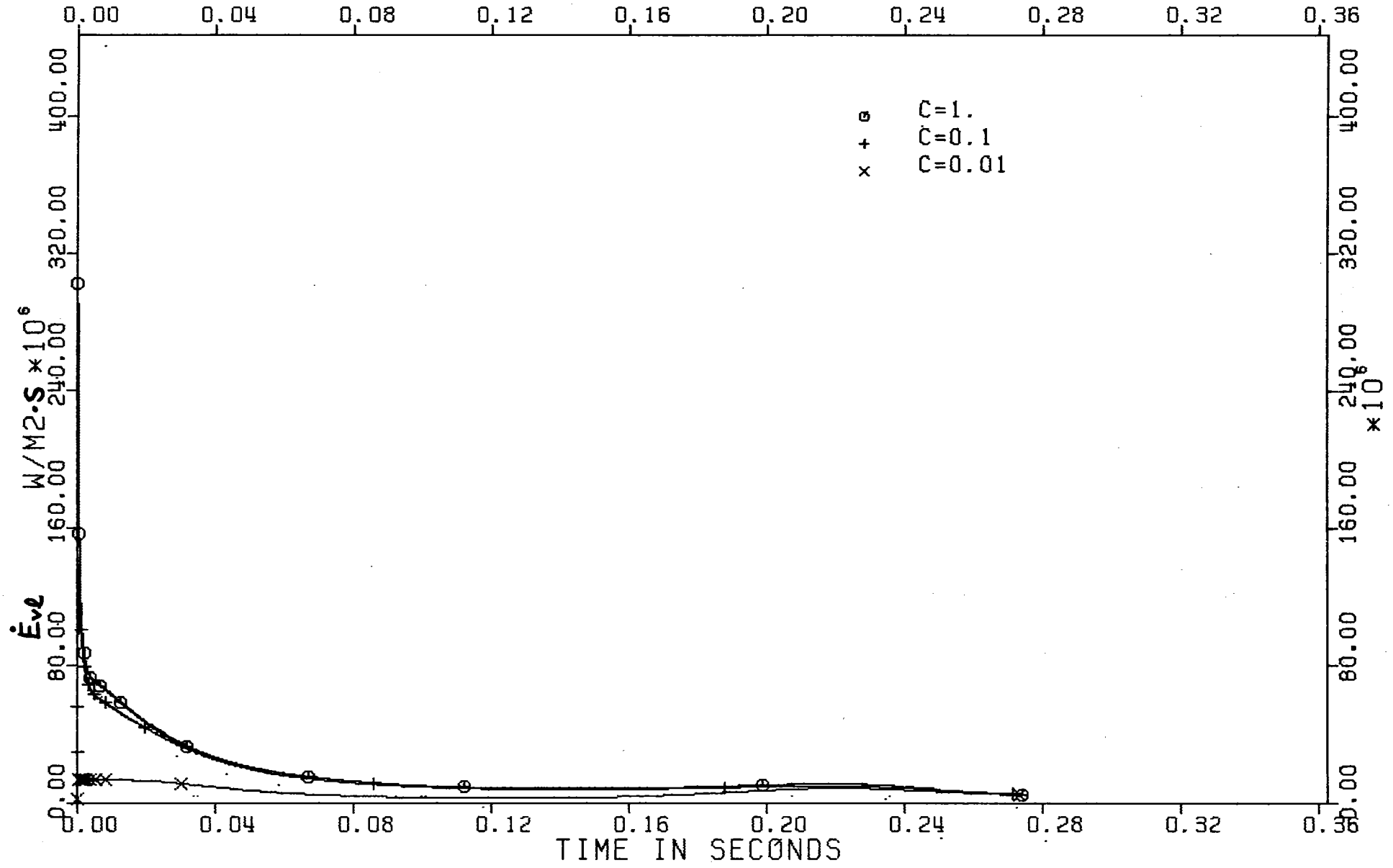

Fig. 10: Comparison of results : energy rate transmitted from the vapor to the liquid ($\dot{E}_{vl}$)

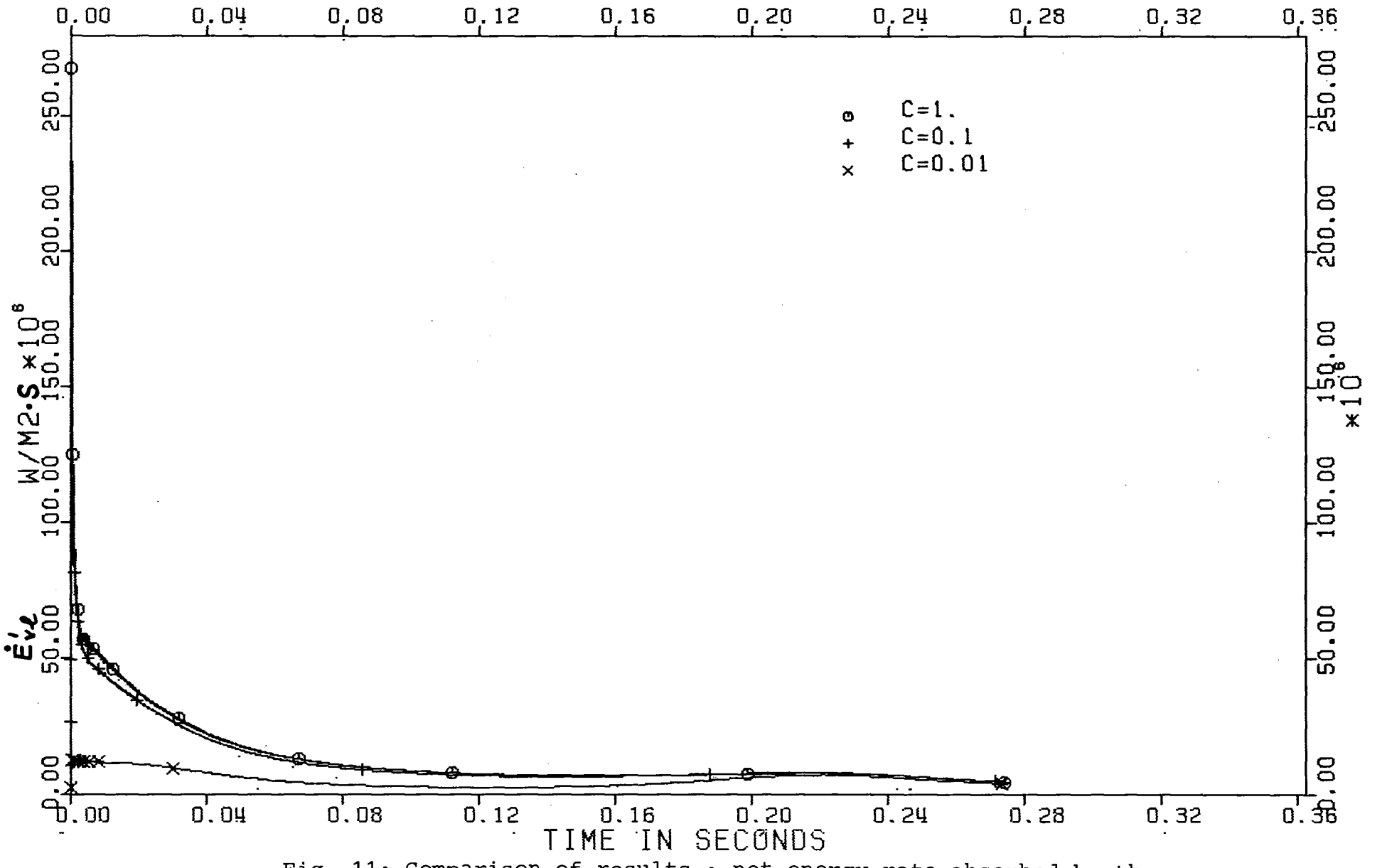

Fig. 11: Comparison of results : net energy rate absorbed by the liquid ($\dot{E}'_{vl}$)

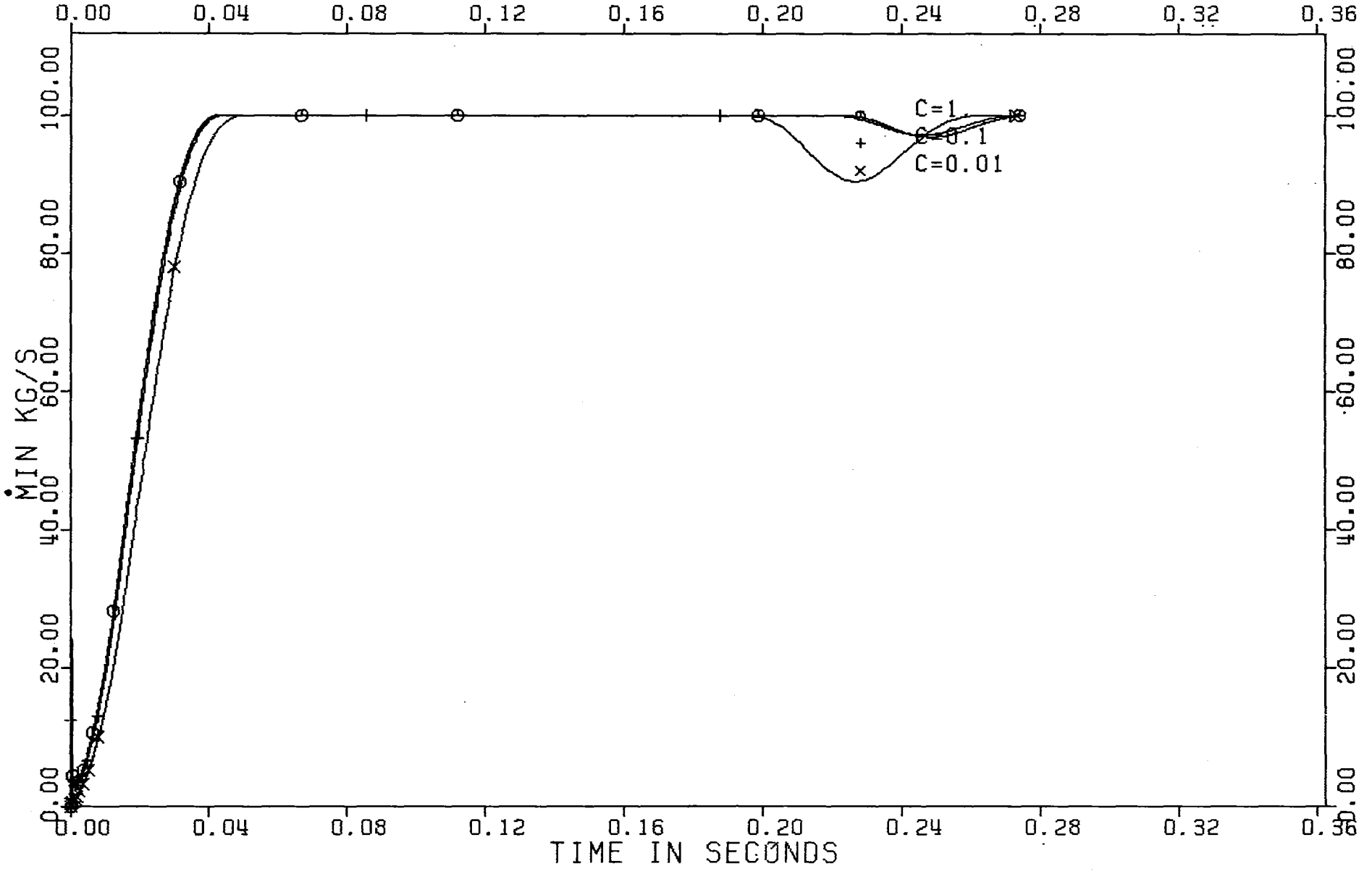

Fig. 12: Comparison of results : introduced mass rate $\dot{M}_{in}$

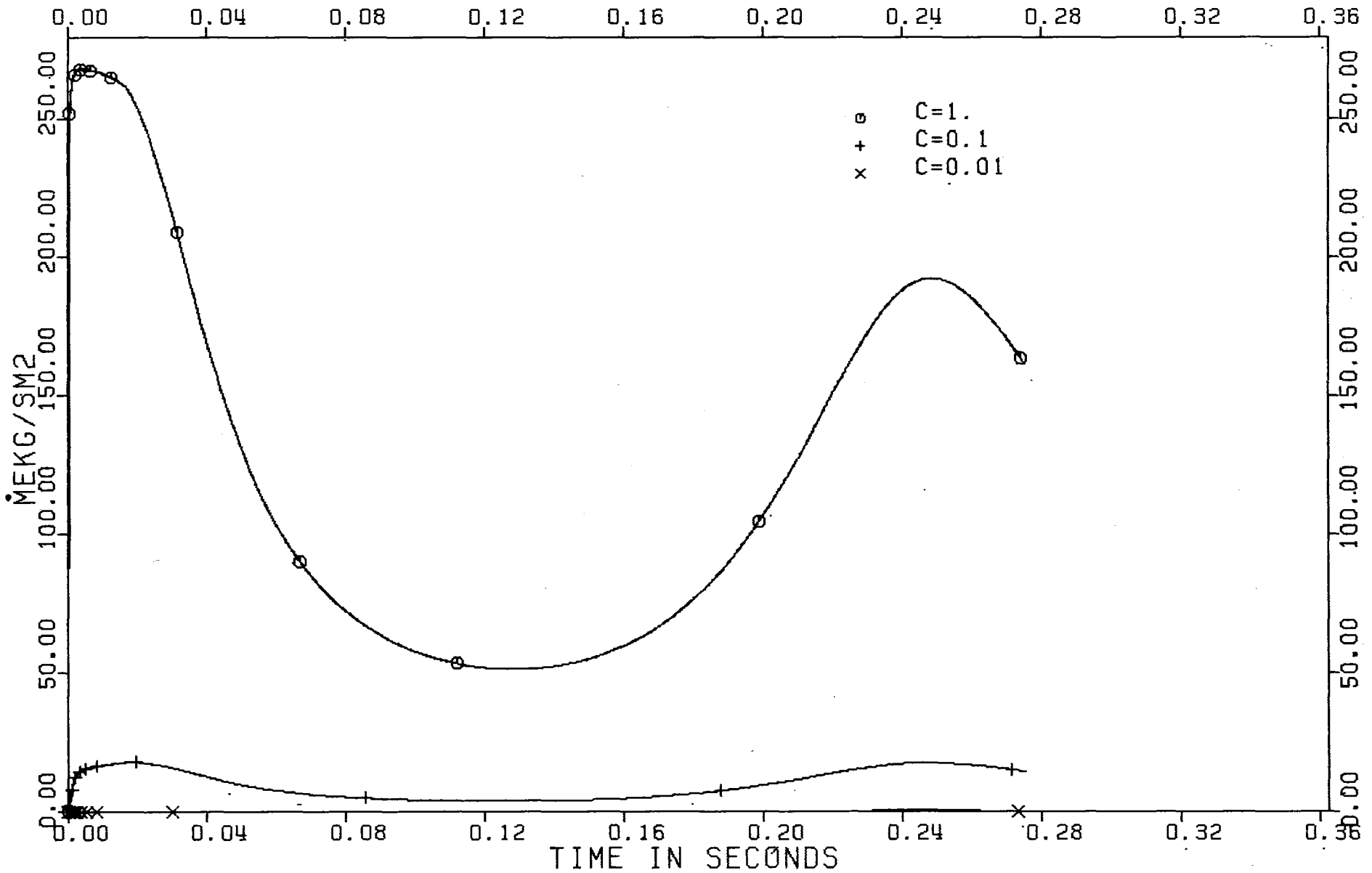

Fig. 13: Comparison of results : evaporated mass rate $\dot{M}_{ev}$

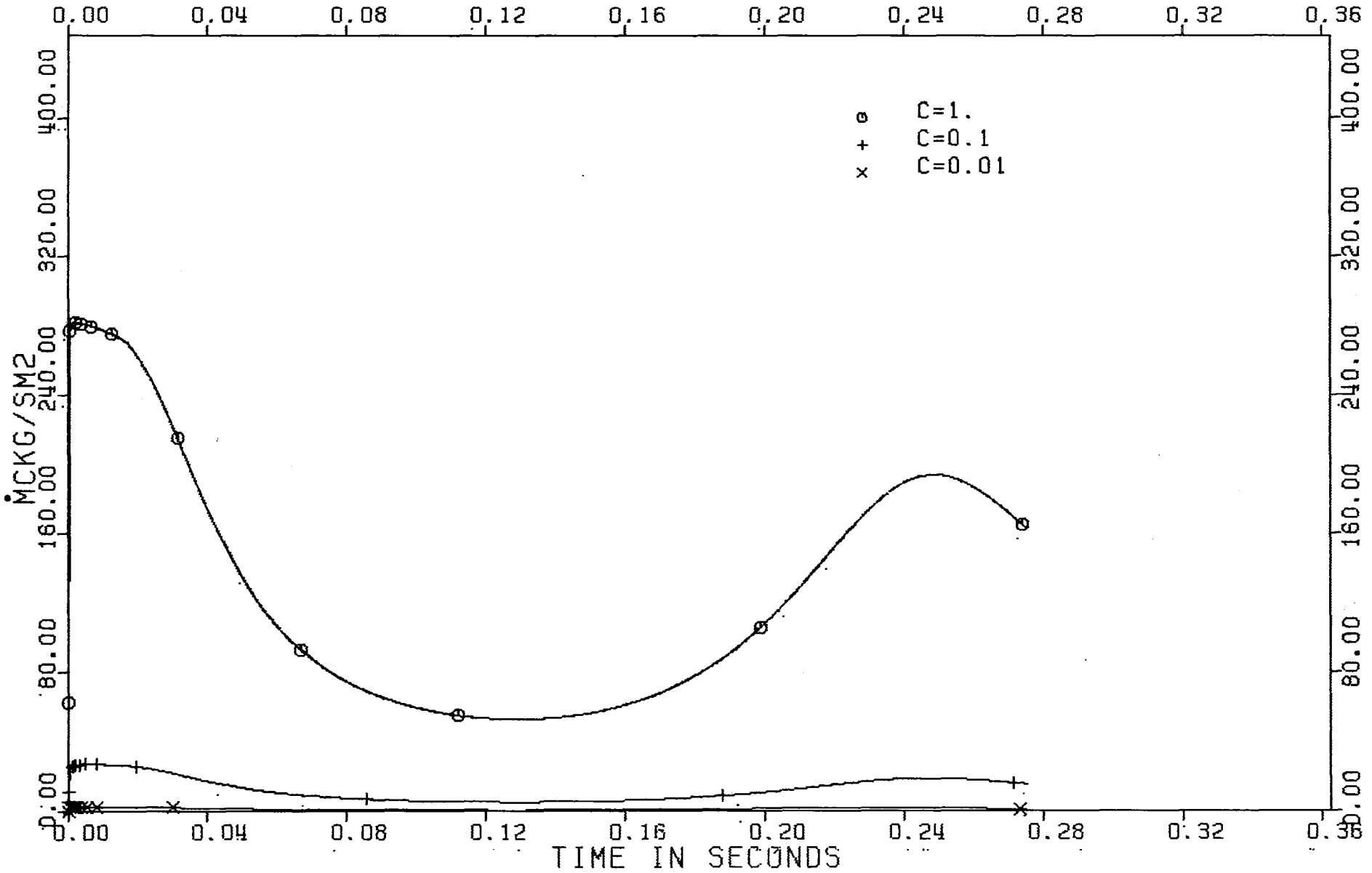

Fig. 14: Comparison of results : condensed mass rate $\dot{M}_{co}$

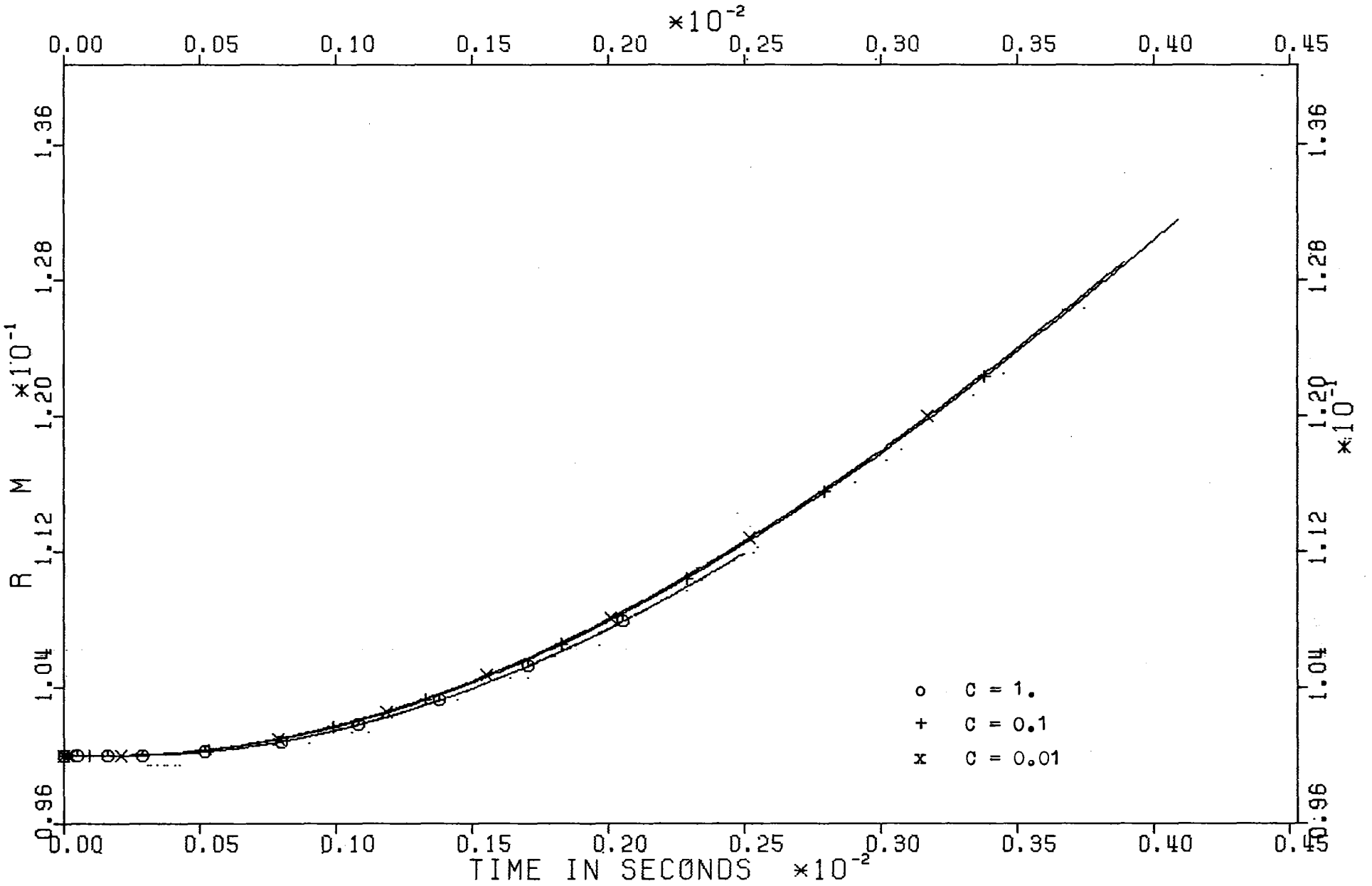

Fig. 15: Comparison of results : bubble radius R

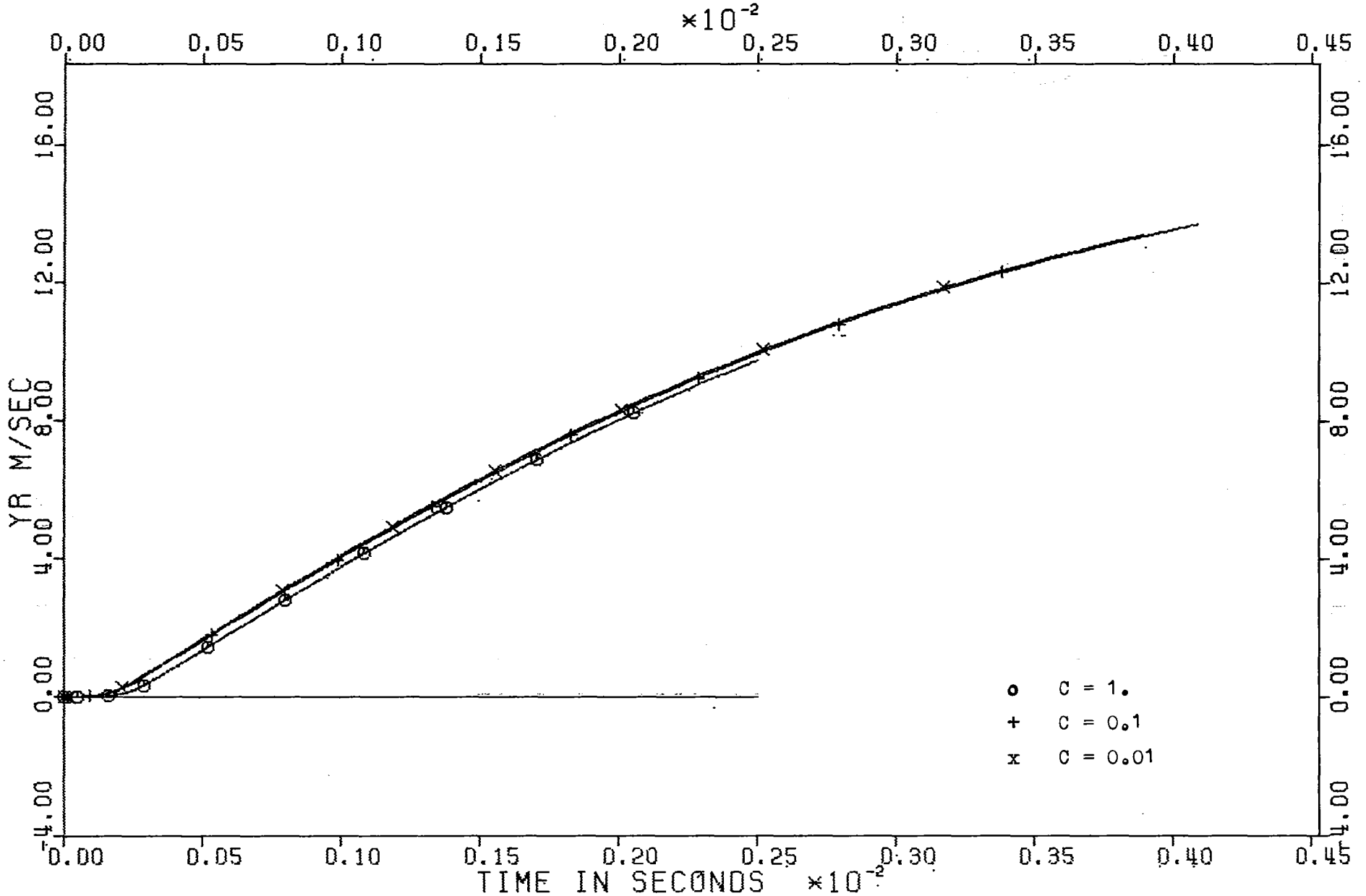

Fig. 16: Comparison of results : bubble growth velocity Y_R

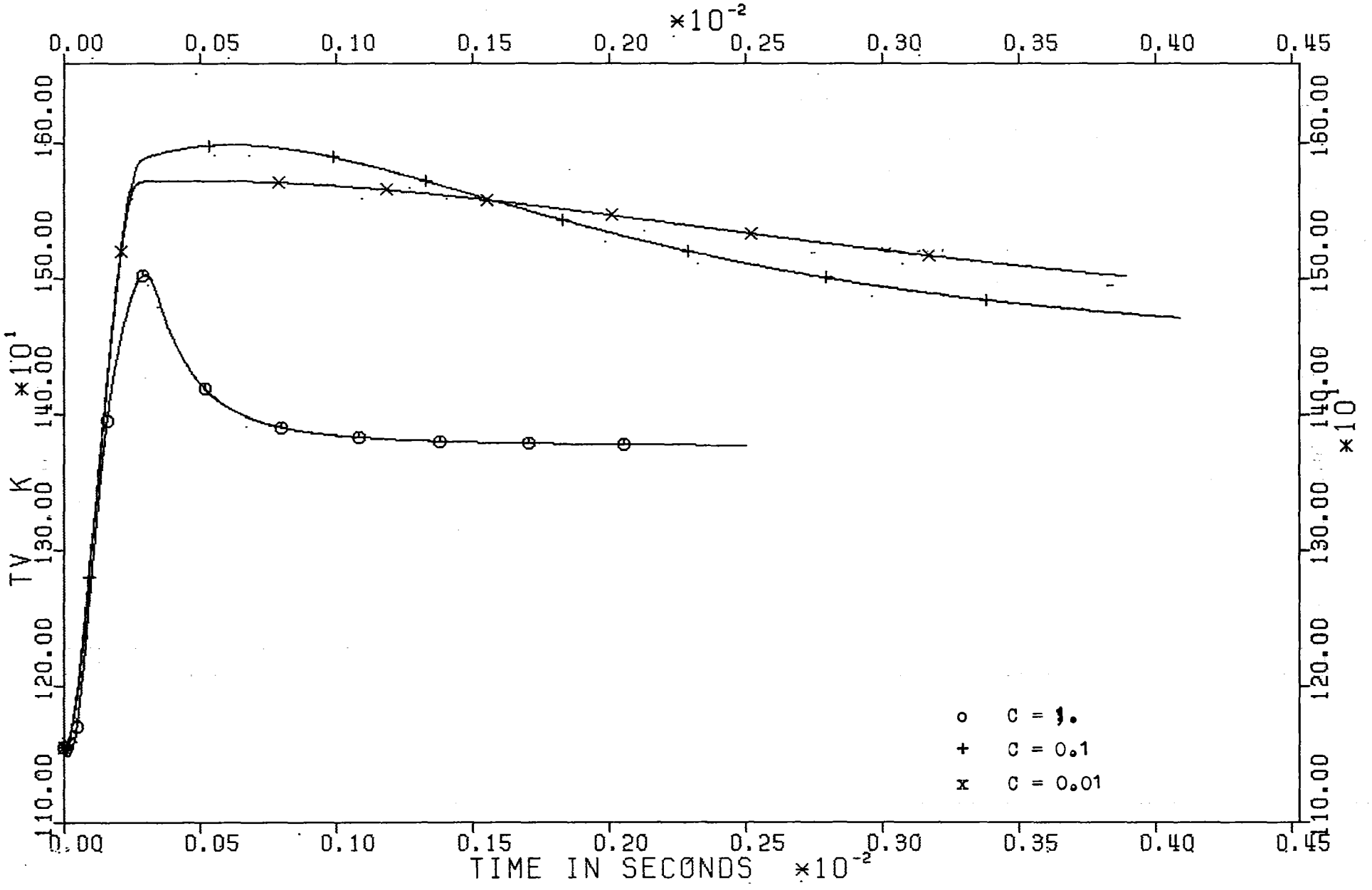

Fig. 17: Comparison of results : bubble vapor temperature T_v

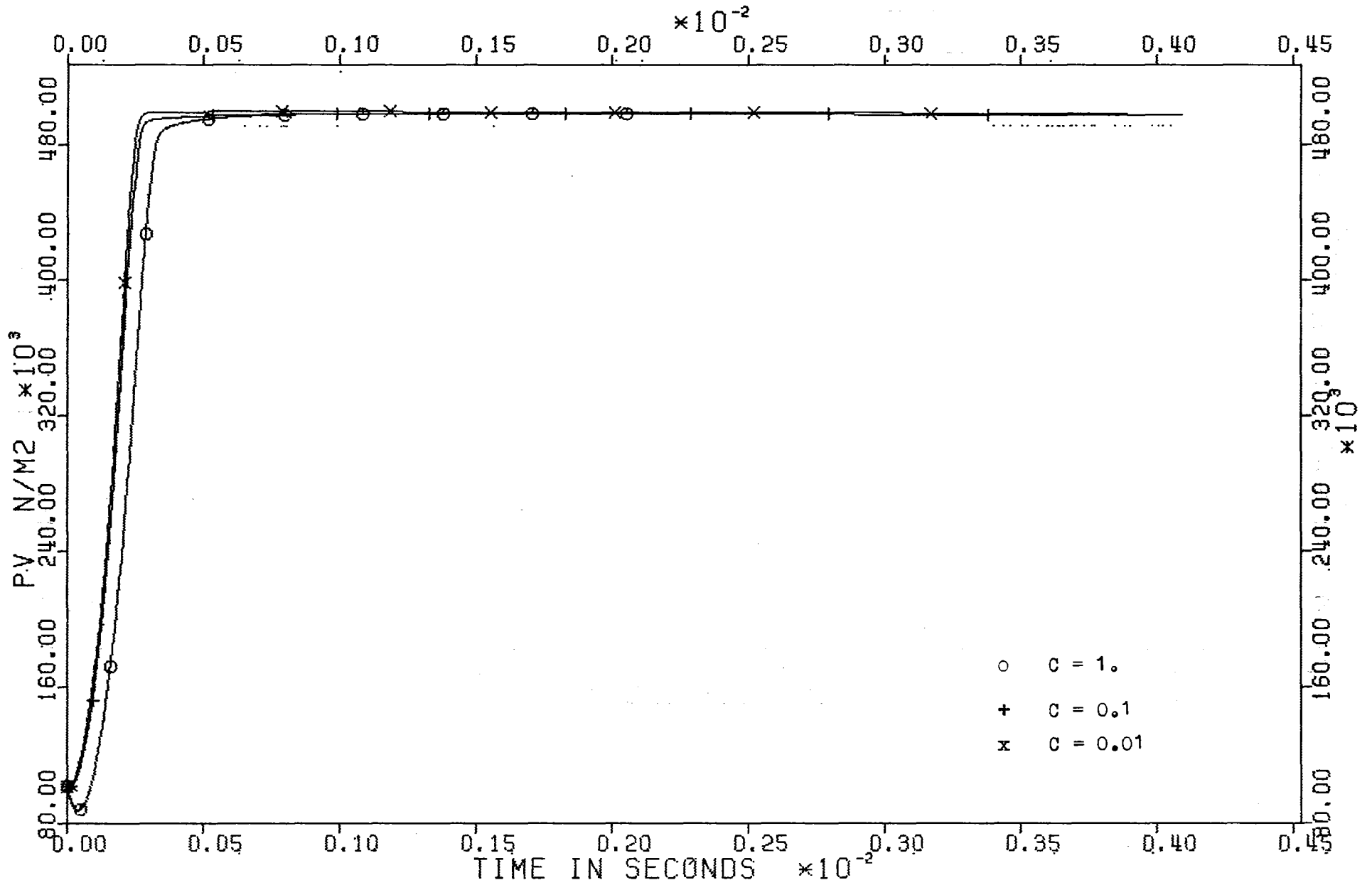

Fig. 18: Comparison of results : bubble pressure p_v

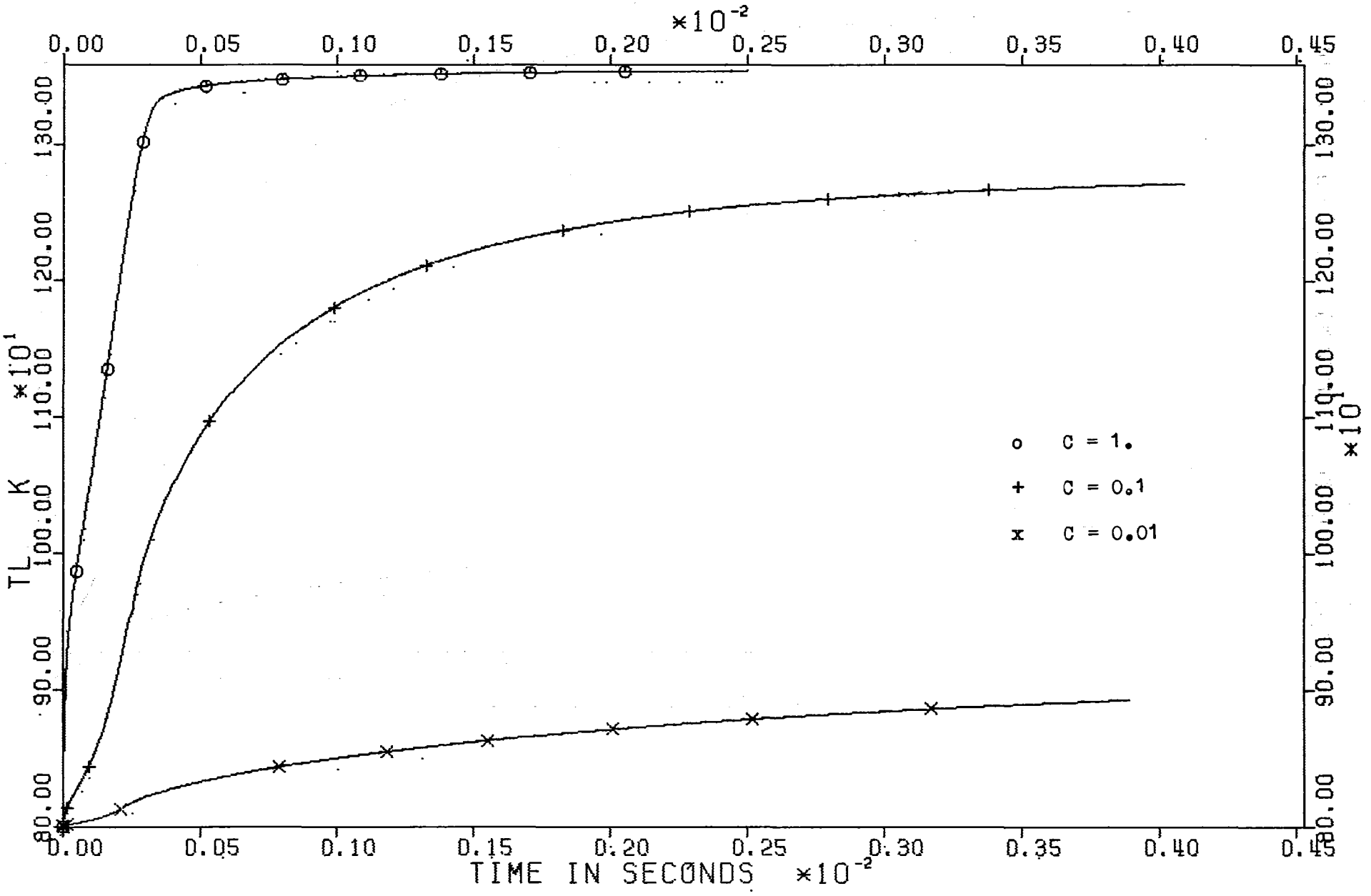

Fig. 19: Comparison of results : liquid interface temperature T_L

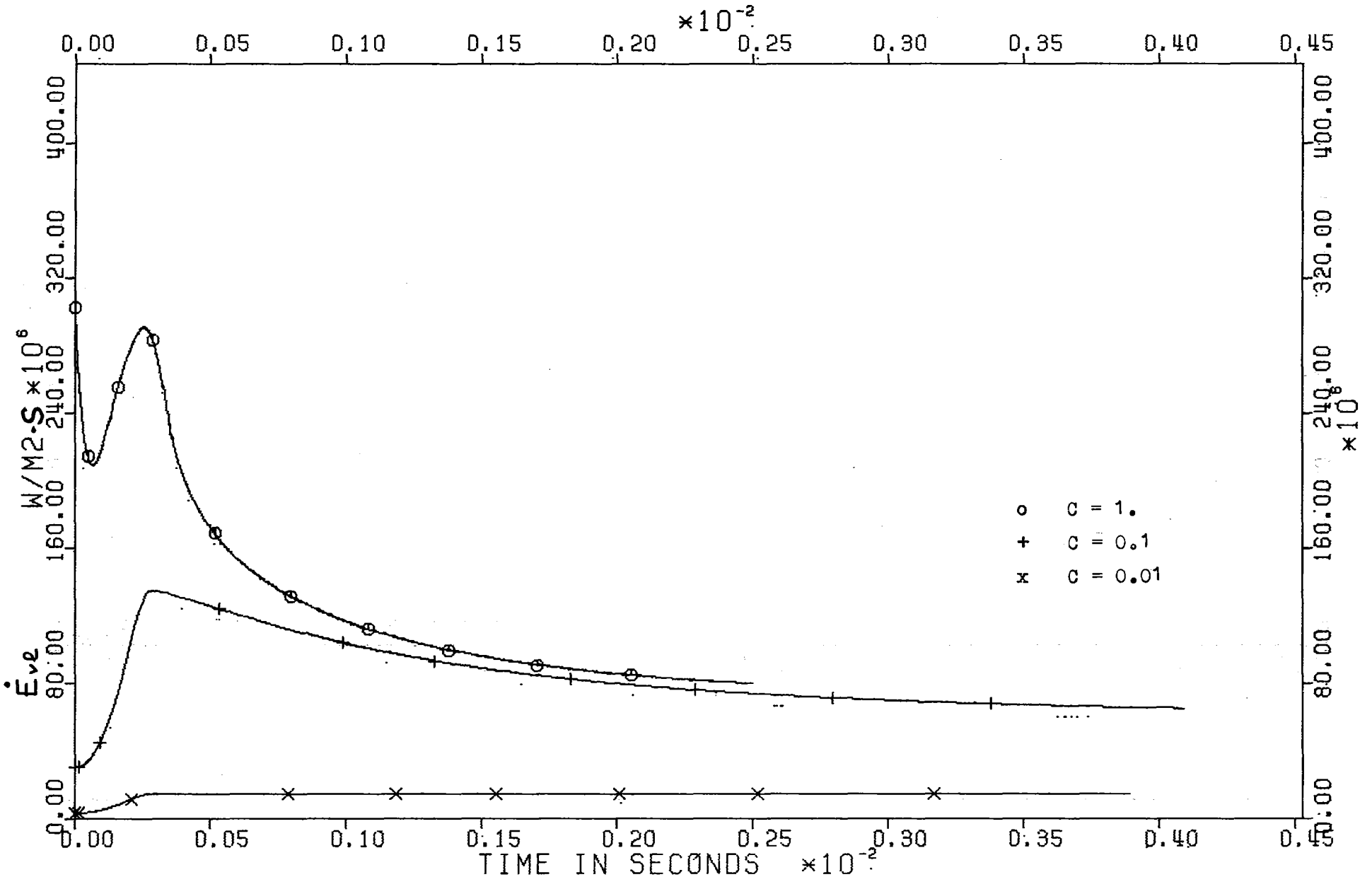

Fig. 20: Comparison of results : energy rate transmitted from the vapor to the liquid ($\dot{E}_{v1}$)

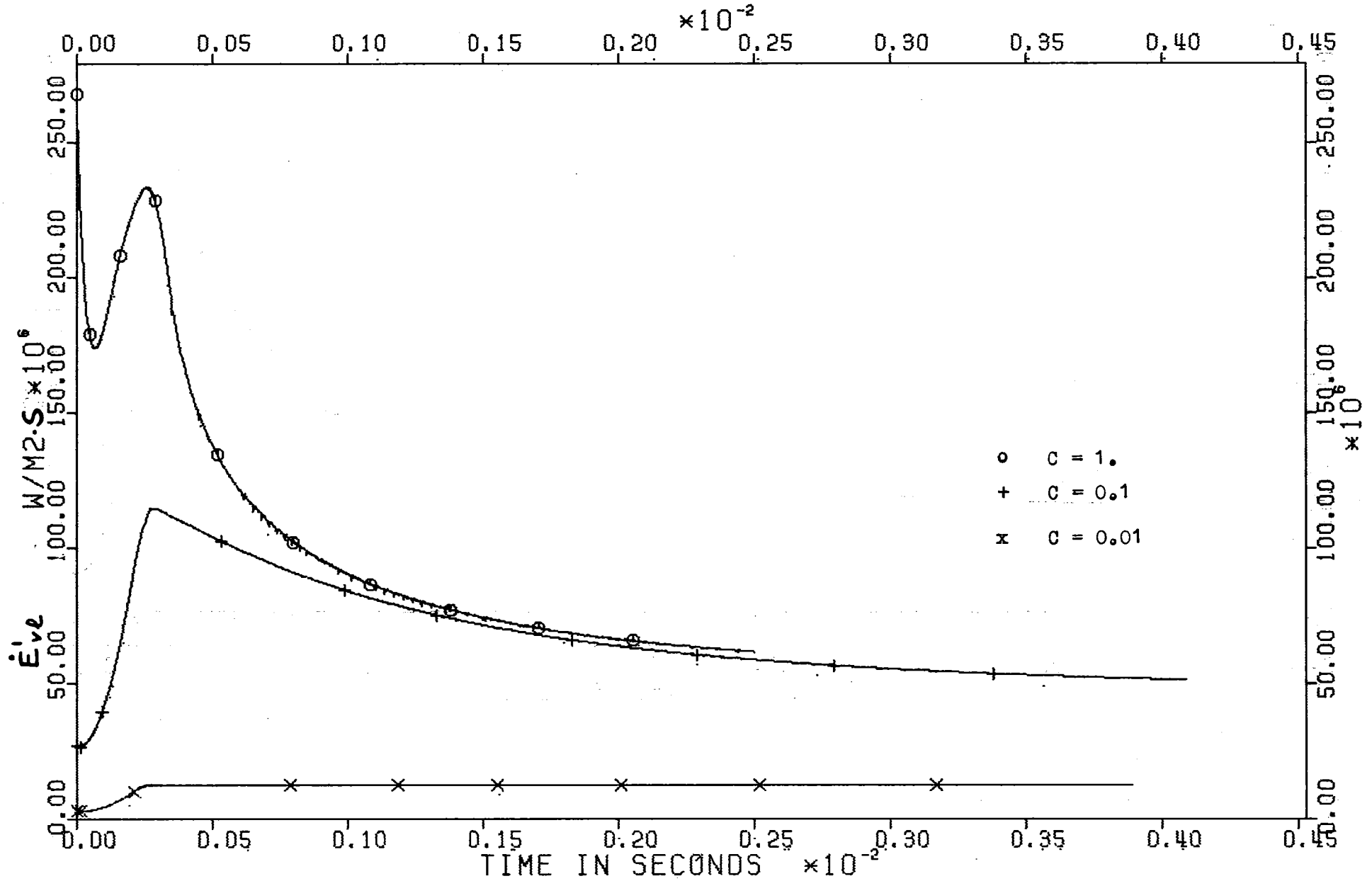

Fig. 21: Comparison of results : net energy rate absorbed by the liquid ($\dot{E}'_{vl}$)

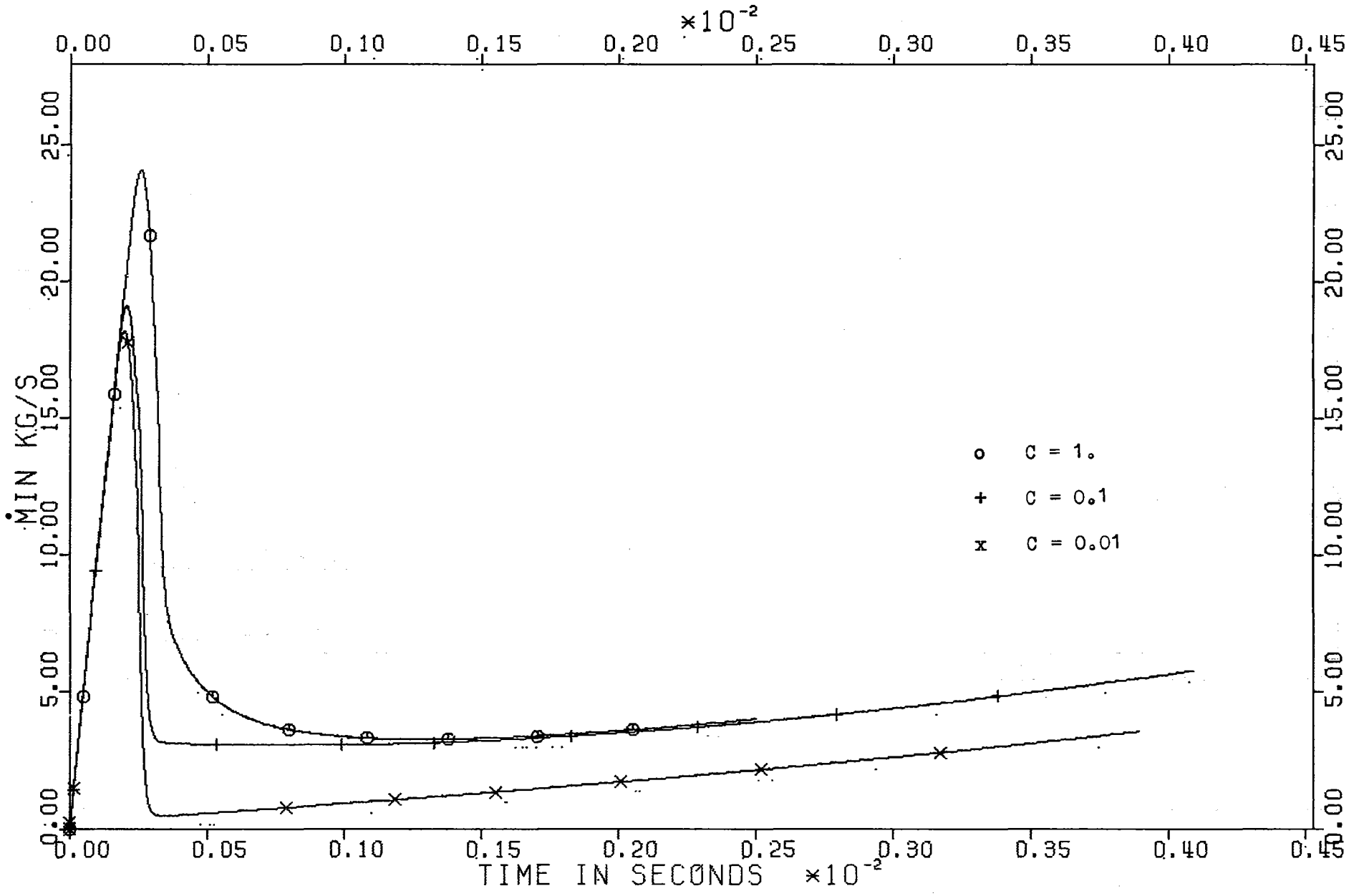

Fig. 22: Comparison of results : introduced mass rate $\dot{M}_{in}$

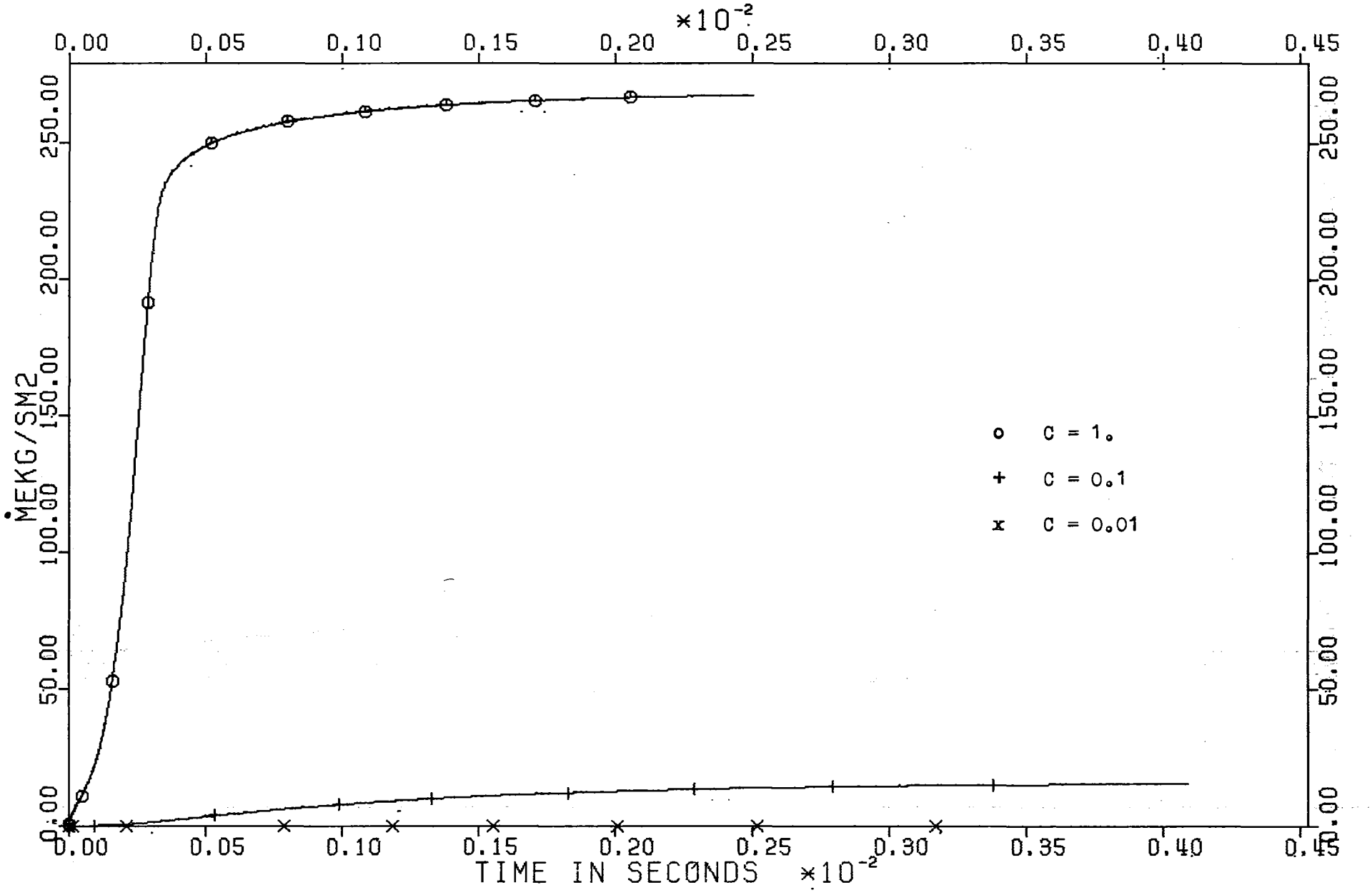

Fig. 23: Comparison of results : evaporated mass rate $\dot{M}_{ev}$

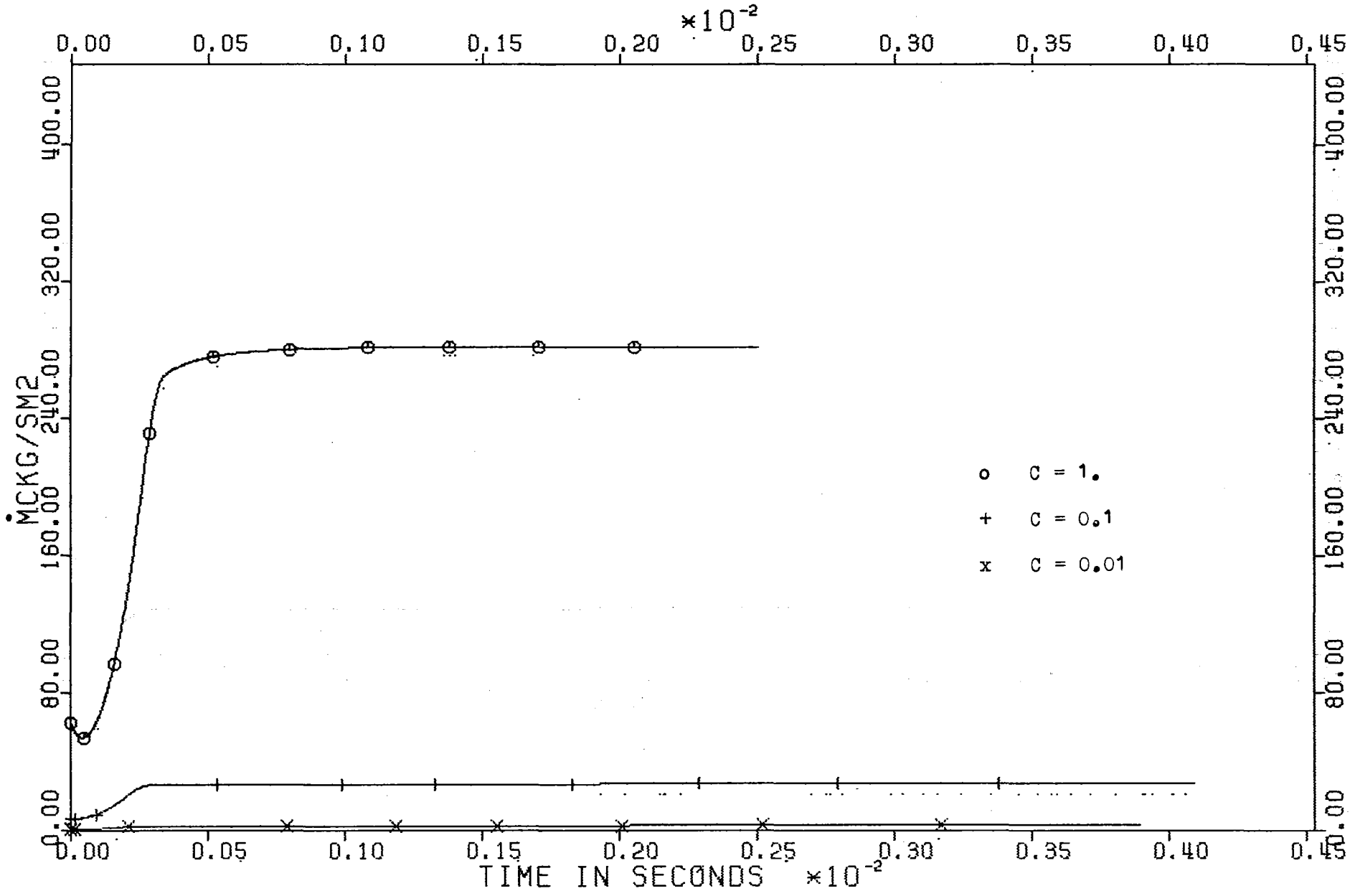

Fig. 24: Comparison of results : condensed mass rate $\dot{M}_{co}$

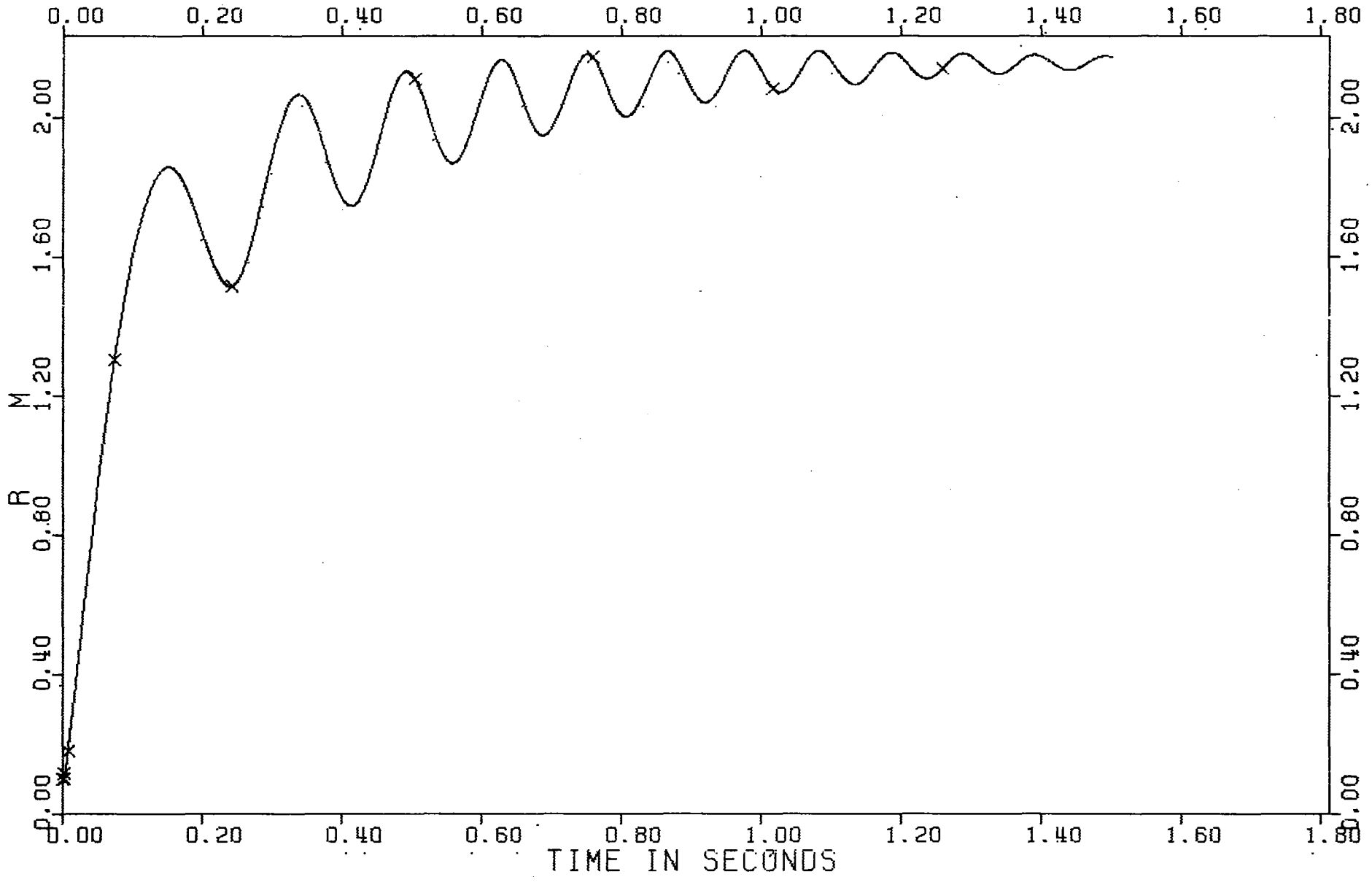

Fig. 25: Case c=0.1. Bubble radius R

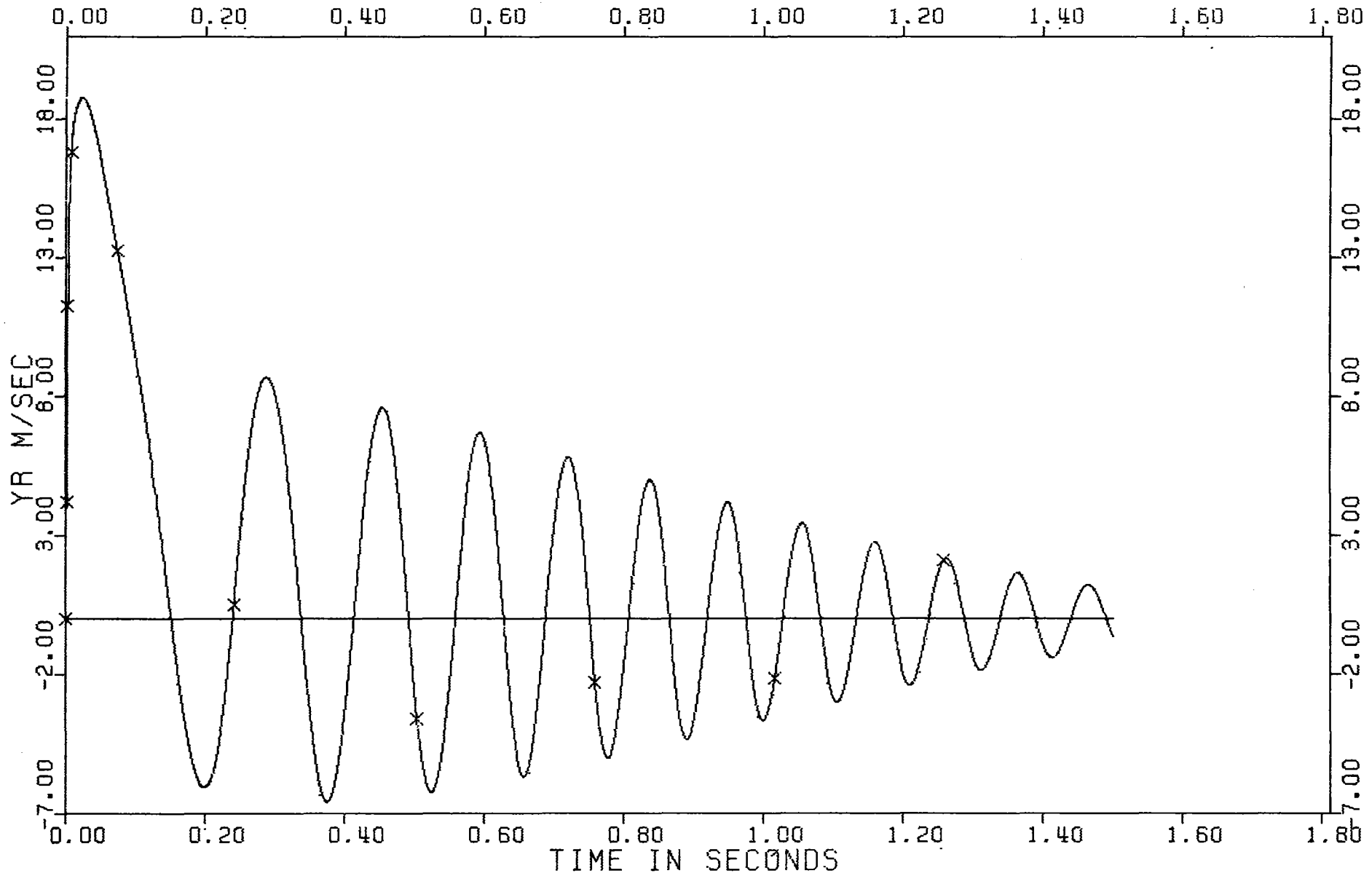

Fig. 26: Case c=0.1 Bubble growth velocity Y_R

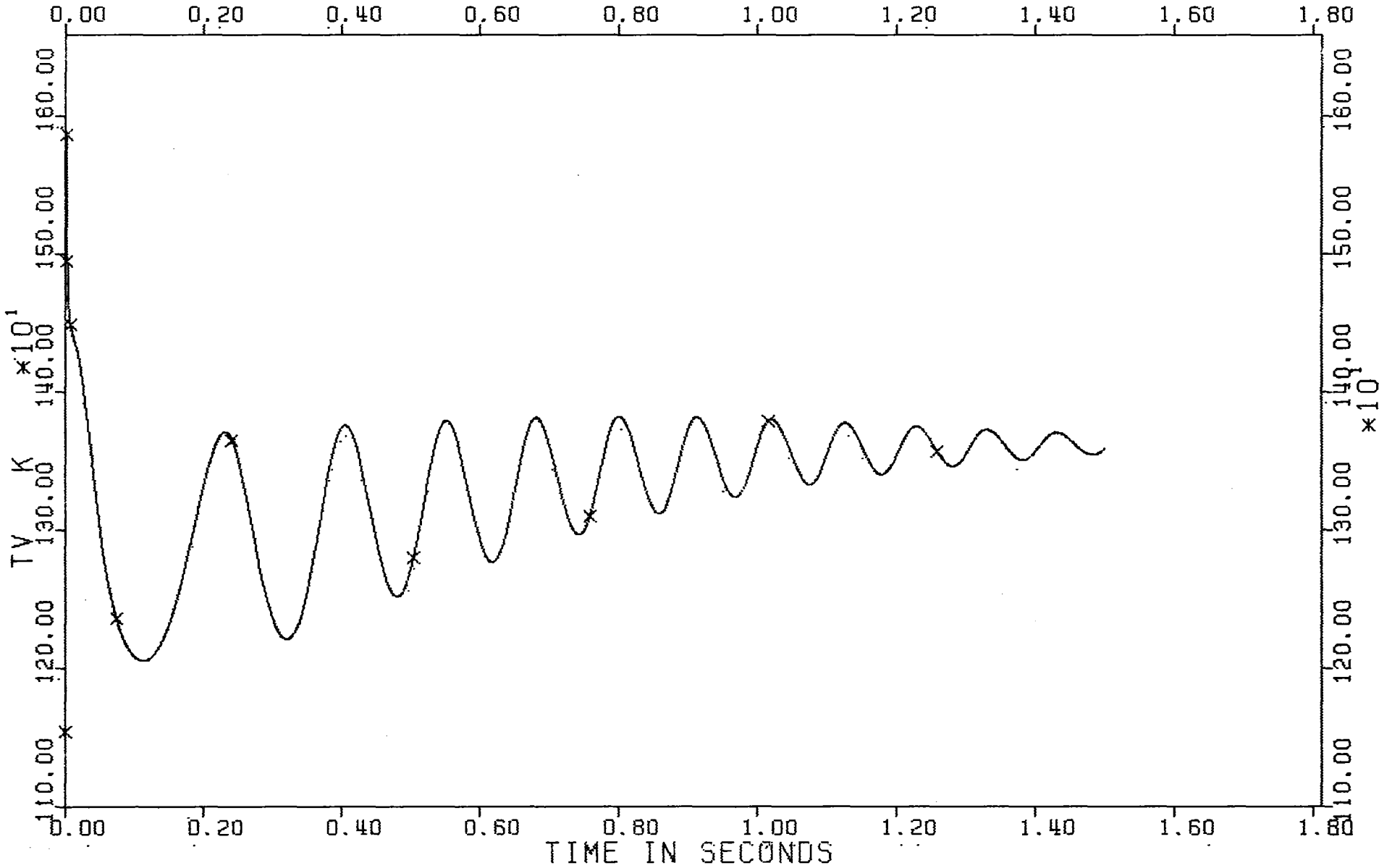

Fig. 27: Case c=0.1 Bubble vapor temperature T_v

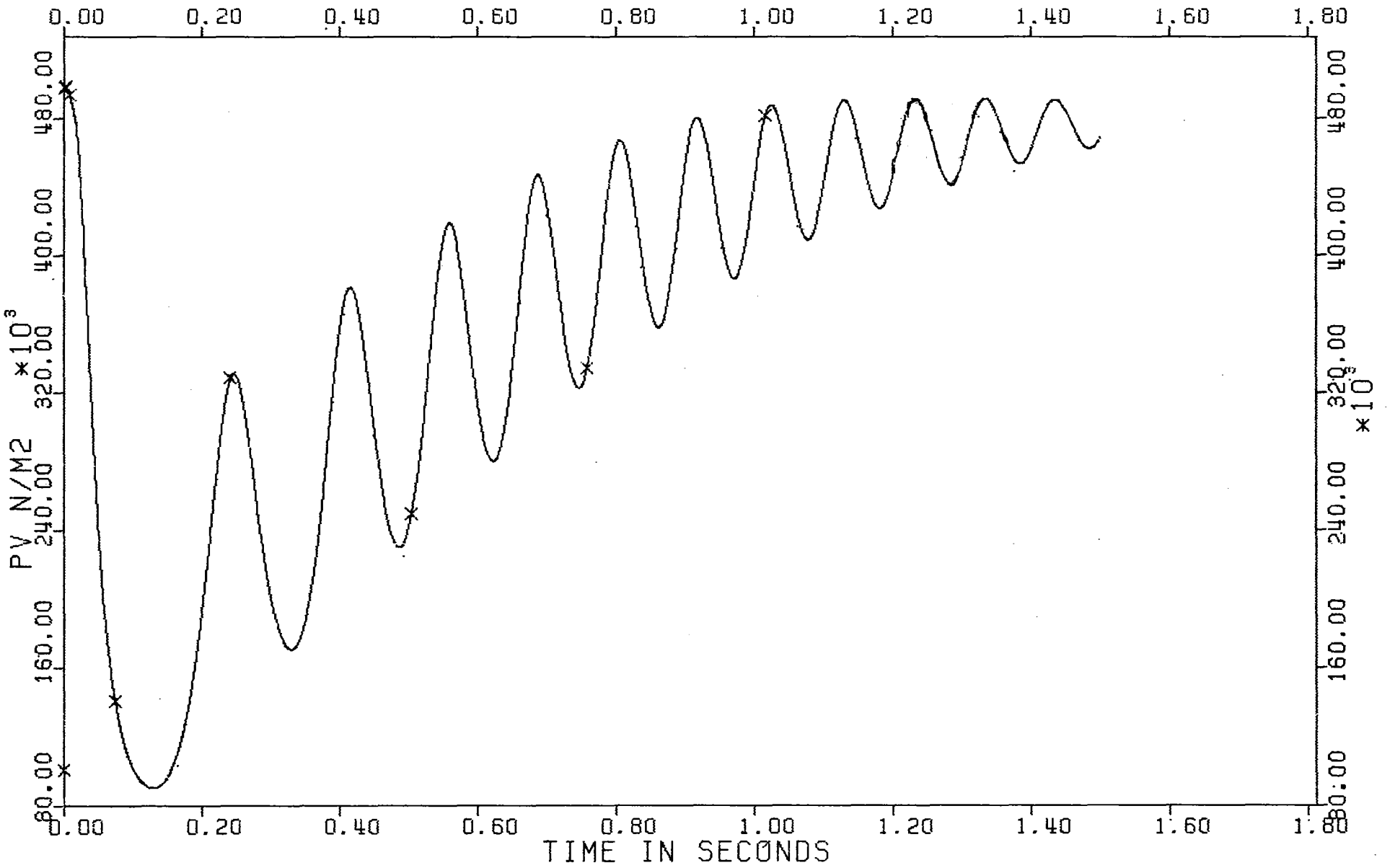

Fig. 28: Case c=0.1. Bubble vapor pressure p_v

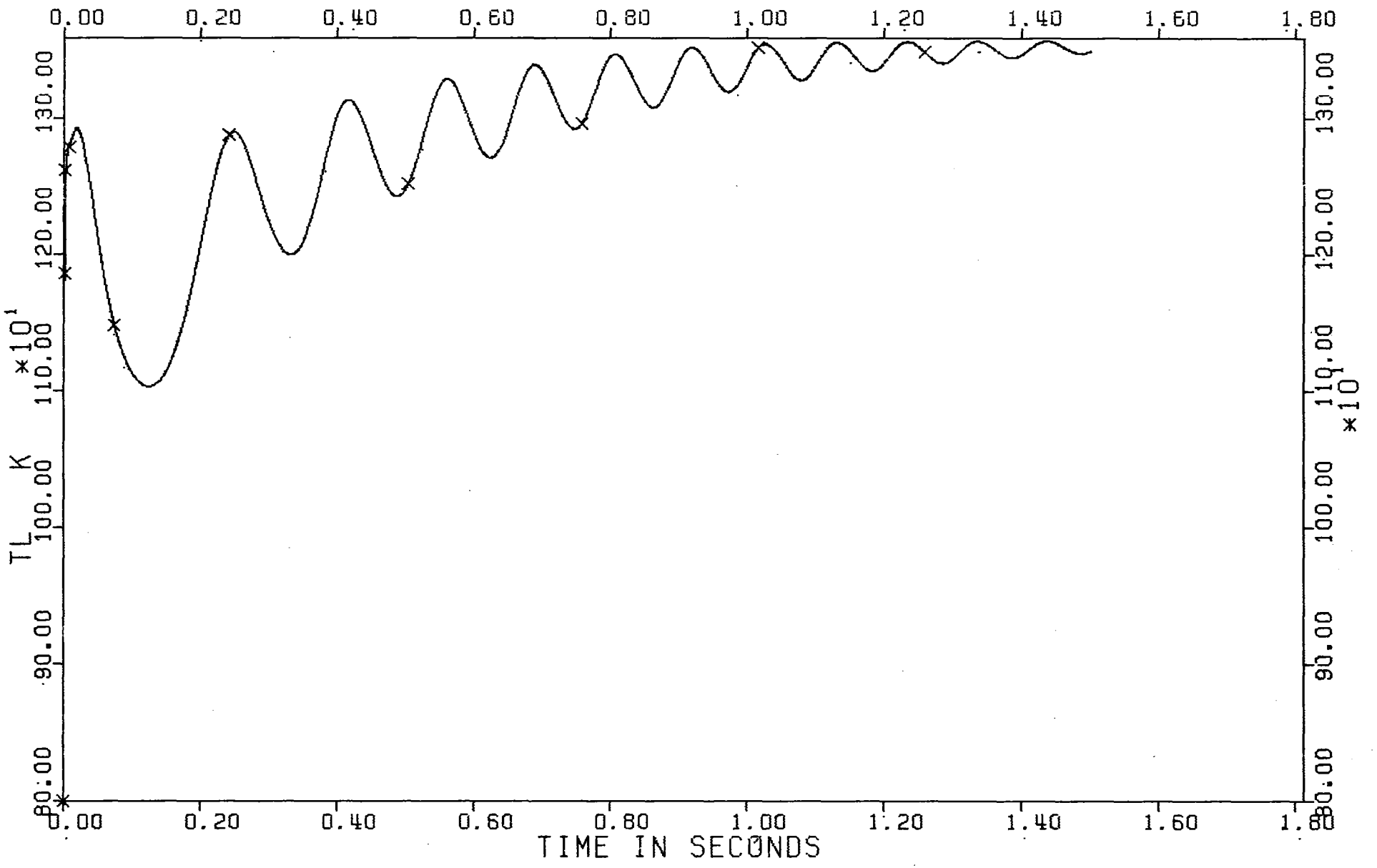

Fig. 29: Case c=0.1 Liquid interface temperature T_L

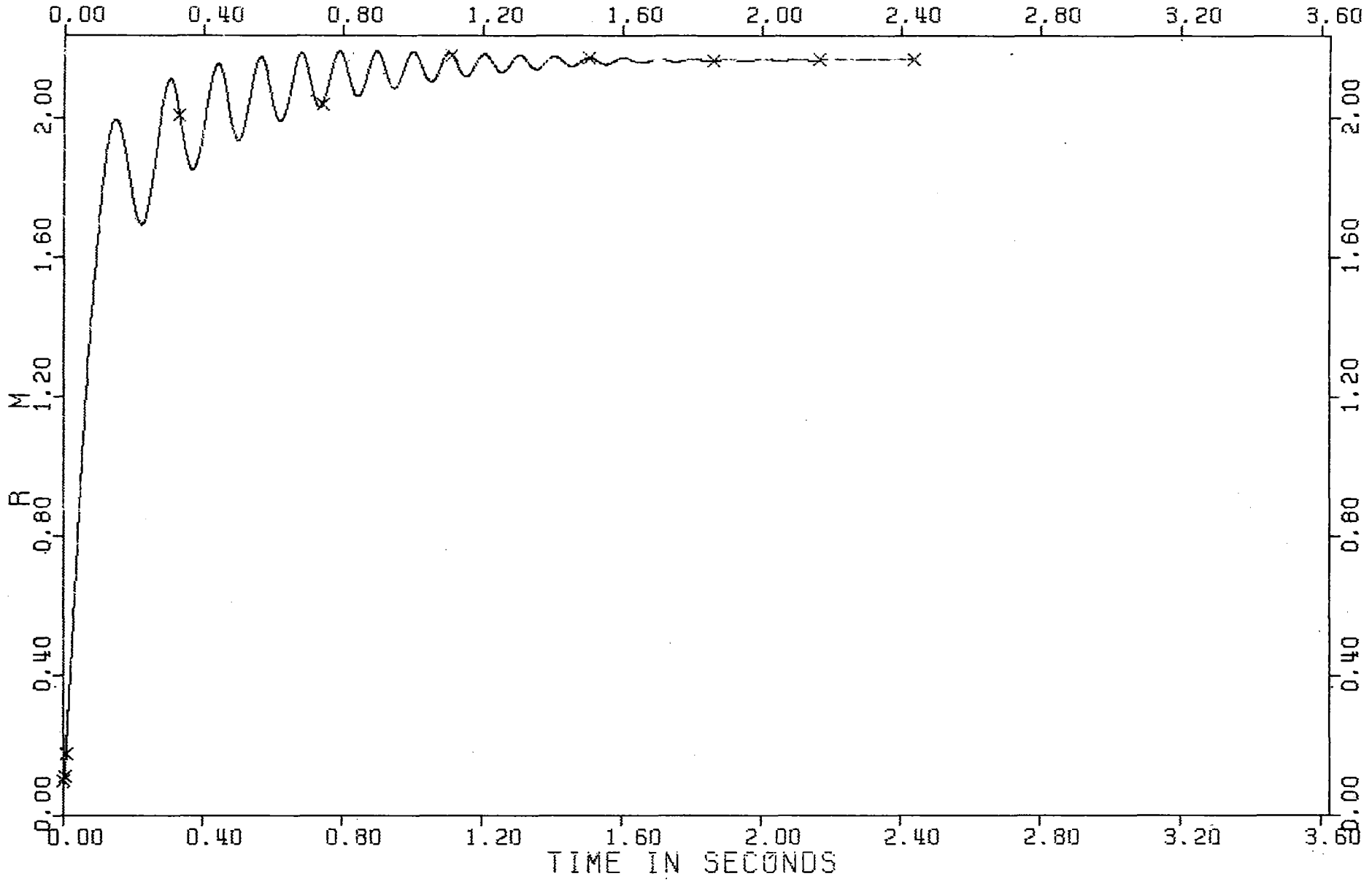

Fig. 30: Case c=0.01. Bubble radius R

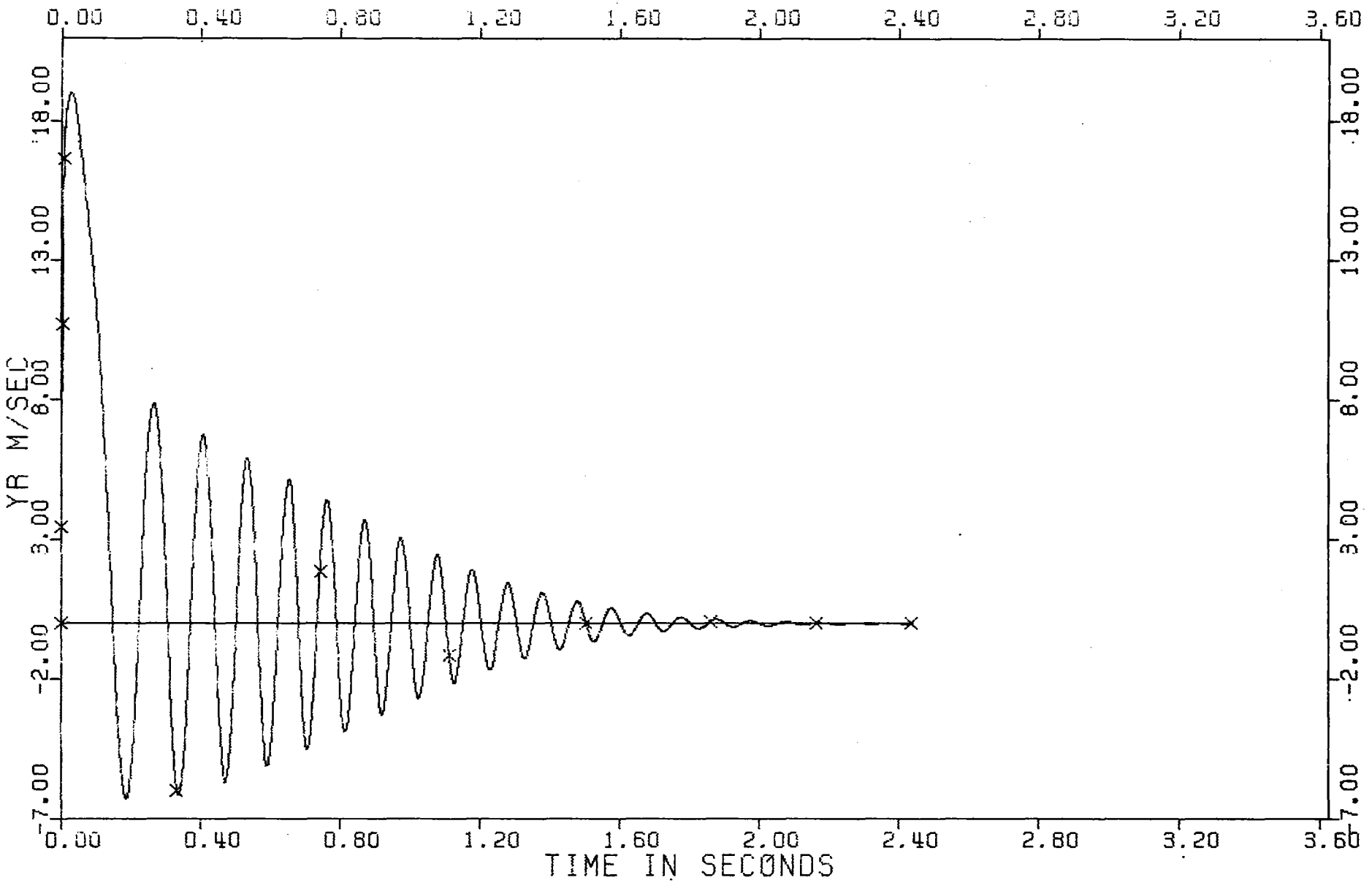

Fig. 31: Case c=0.01. Bubble velocity Y_R

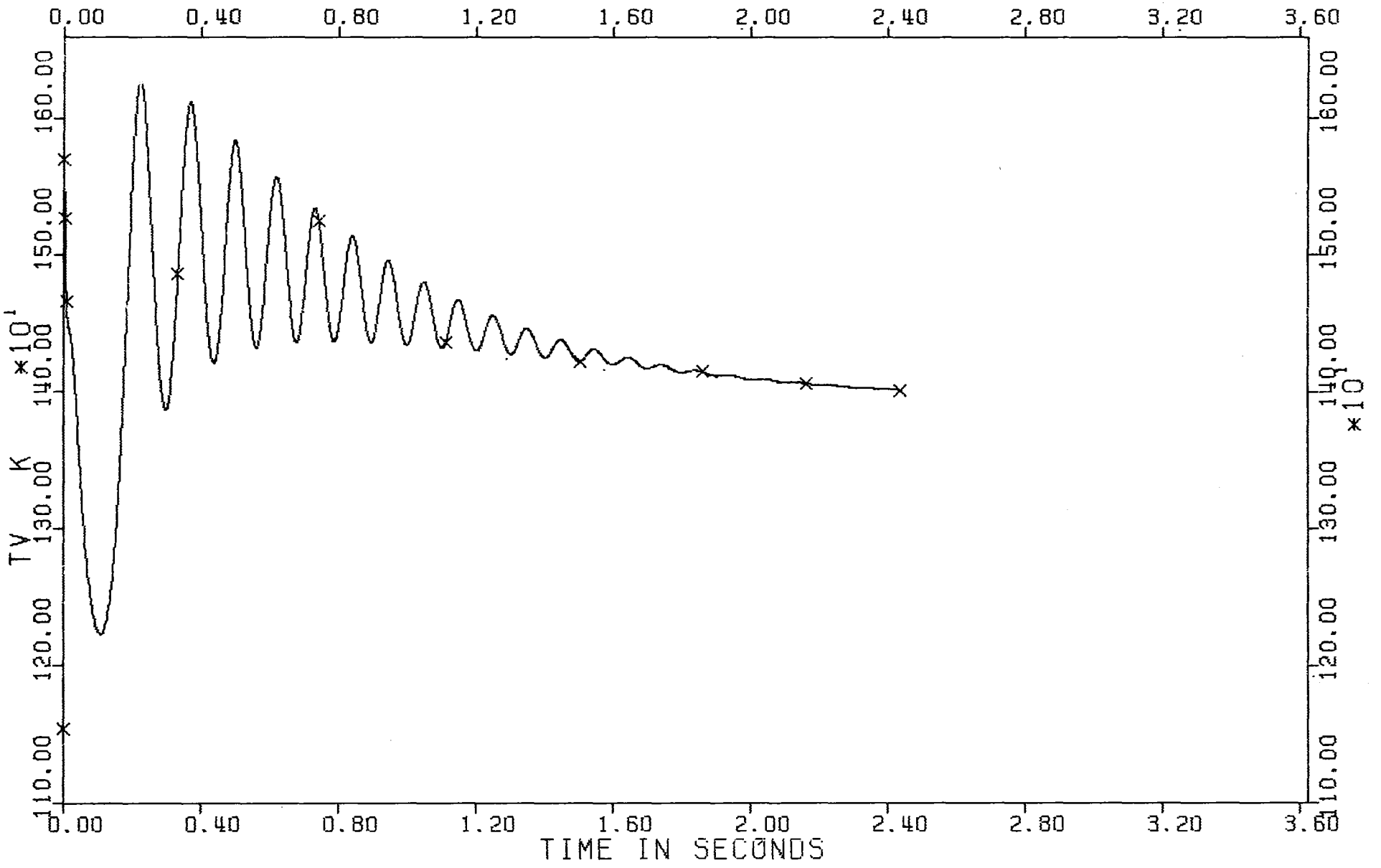

Fig. 32: Case c=0.01. Bubble vapor temperature T_v

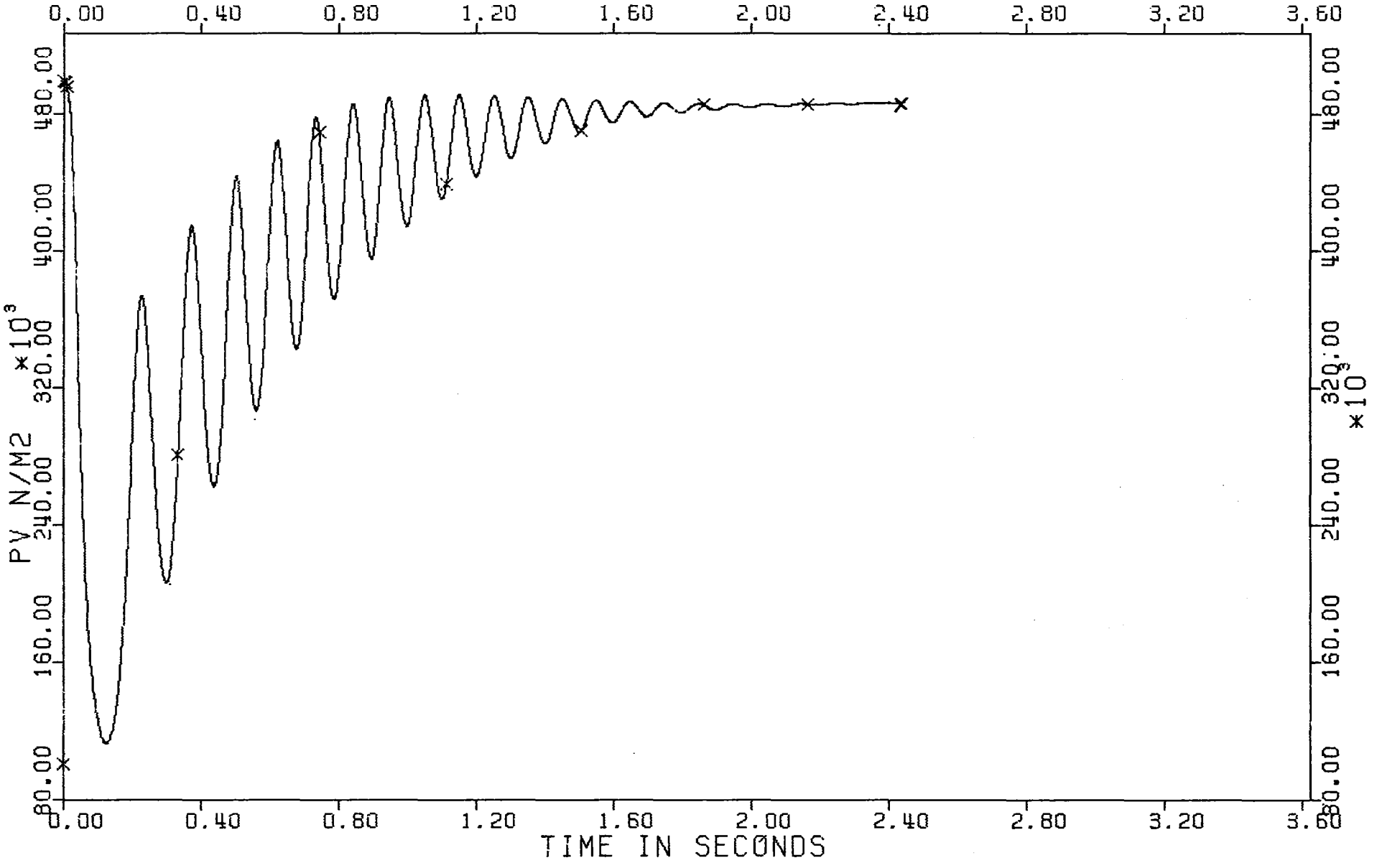

Fig. 33: Case c=0.01. Bubble vapor pressure p_v

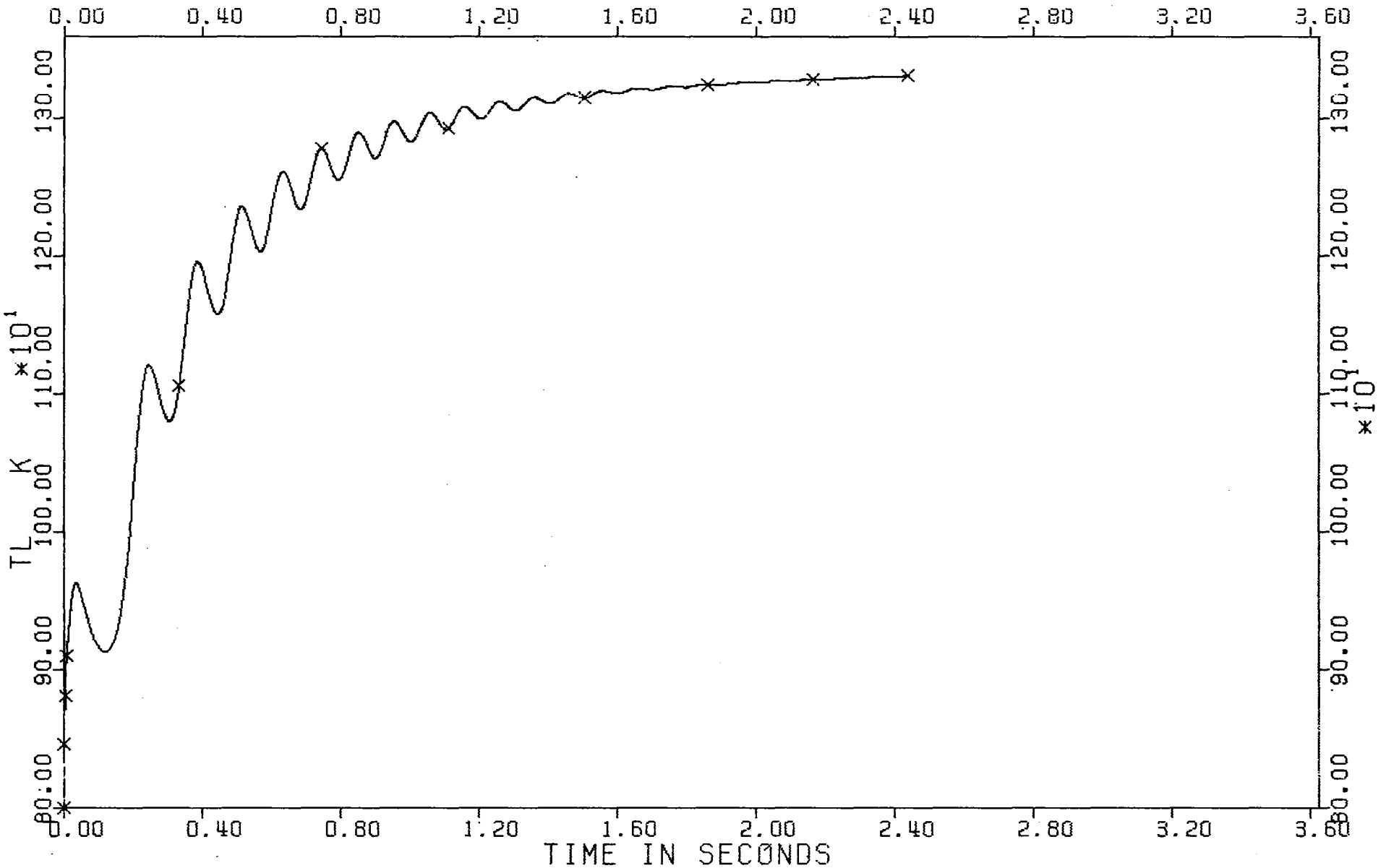

Fig. 34: Case c=0.01. Liquid interface temperature T_L